



**HAL**  
open science

## Release of labile Si from forest and agricultural soils

Artem Lim, Oleg Pokrovsky, Sophie S. Cornu, Jean-Dominique Meunier

► **To cite this version:**

Artem Lim, Oleg Pokrovsky, Sophie S. Cornu, Jean-Dominique Meunier. Release of labile Si from forest and agricultural soils. *CATENA*, 2023, 229, pp.107211. 10.1016/j.catena.2023.107211 . hal-04167051

**HAL Id: hal-04167051**

**<https://hal.science/hal-04167051v1>**

Submitted on 21 Jul 2023

**HAL** is a multi-disciplinary open access archive for the deposit and dissemination of scientific research documents, whether they are published or not. The documents may come from teaching and research institutions in France or abroad, or from public or private research centers.

L'archive ouverte pluridisciplinaire **HAL**, est destinée au dépôt et à la diffusion de documents scientifiques de niveau recherche, publiés ou non, émanant des établissements d'enseignement et de recherche français ou étrangers, des laboratoires publics ou privés.

# 1                   **Release of labile Si from forest and agricultural soils**

2  
3       Artem G. Lim<sup>1</sup>, Oleg S. Pokrovsky<sup>1,2,3\*</sup>, Sophie Cornu<sup>4</sup>, Jean-Dominique Meunier<sup>4</sup>

4  
5       <sup>1</sup> *BIO-GEO-CLIM Laboratory, Tomsk State University, 36 Lenina Prs, 634050, Tomsk,*  
6       *Russia*

7       <sup>2</sup> *GET, CNRS - University of Toulouse, 14 Avenue Edouard Belin, 31400 Toulouse, France*

8       <sup>3</sup> *N. Laverov Federal Center for Integrated Arctic Research, UrB RAS, 23 Nab Severnoi*  
9       *Dviny, Arkhangelsk, 163000, Russia*

10       <sup>4</sup> *CEREGE, Aix-Marseille University, CNRS, IRD, INRAE, BP 80, 13545 Aix-en-Provence,*  
11       *France*

12  
13       \* oleg.pokrovsky@get.omp.eu

14  
15  
16  
17  
18       Submitted to *Catena* after revision, *May 2023*

19  
20       Keywords: soil, forest, silicate, silica, dissolution, kinetics, rates, labile pool

29 **Abstract**

30 Despite the importance of silicon (Si) as beneficial nutrient for many plants, including  
31 economically-important cereals, the reactivity of various Si pools in soils (silicate minerals,  
32 amorphous compounds, phytoliths, organic litter) is not fully quantified which does not allow  
33 predicting the capacity of agricultural or forested soil to provide soluble Si to soil porewaters  
34 where it can be used by plants. Towards better understanding of factors controlling  
35 bioavailable Si in soils, here we quantified the release rate of Si from several pairs of French  
36 forest and agricultural topsoils, developed on calcareous or loess parent material. We used  
37 mixed-flow and column reactors, in acetate and carbonate buffers and distilled water, at  
38 various pH (4 to 8) and time of reaction (day to month).

39 The rate of Si release from soil ( $R_{Si}$ ) exceeded that of crystalline clay minerals by 1 to 2  
40 orders of magnitude, being 5 to 10 times lower than that of various allophanes. The rates were  
41 weakly dependent on pH (compared to clays or phytoliths) and varied from  $5 \times 10^{-7}$  to  $2 \times 10^{-6}$   
42 mol/g<sub>soil</sub>/day at  $4 < \text{pH} \leq 8$ . In terms of Si reactivity, four studied soil groups followed the  
43 order: “calcaric cambisols  $\approx$  hypereutric cambisols  $\geq$  luvisols  $\geq$  albeluvisol”. Calcaric and  
44 hypereutric cambisols as well as luvisols exhibited a weak decrease of  $R_{Si}$  with pH increase.  
45 The rate of Si release from albeluvisol increased 2 times with a pH increase from 4 to 8.  
46 There was no measurable difference in  $R_{Si}$  between agricultural and forest soils.

47 The pool of labile Si in forest soils was quantified via soil column flow-through  
48 experiments. The breakthrough curves of Si demonstrated high concentrations (1.6 to 5.7  
49 mg/L) over first several hours of reaction in the soil column. The water leachable Si pool  
50 ranged from 0.04 to 0.08 mg Si g<sub>soil</sub><sup>-1</sup>, corresponding to labile Si stock in the 0-20 cm soil of  
51 80 to 160 kg ha<sup>-1</sup>. These values can meet the annual requirements of plants in forests and  
52 cultivated soils. The pool of labile Si correlated ( $R_{\text{Pearson}} > 0.90$ ;  $p < 0.05$ ) with Si associated  
53 with amorphous Fe and Al compounds and soluble bioavailable Si extracted using CaCl<sub>2</sub>

54 method, but negatively correlated with total Si content in soils and Si of phytoliths. The main  
55 pools of soil labile Si could be allophanes, organo-Fe-Al-Si compounds and adsorbed forms  
56 of Si onto Fe and Al hydroxides. We hypothesize that, because of low sensibility of  $R_{Si}$  to  
57 type of soil and fluid pH, the majority of soils regulate Si release at some ‘universal’ rate  
58 which is further reflected in relatively narrow range of riverine Si concentrations and export  
59 fluxes across the world. Therefore, the modeling of chemical weathering and element export  
60 flux in the watersheds should incorporate the experimentally measured reactivity of the whole  
61 soil rather than individual constituting primary or secondary minerals.

62

63

## 64 **1. Introduction**

65 Silicon is not seen as an essential element for plants, but many studies have  
66 documented that it is a beneficial element for many crops (Coskun et al., 2019). Low level of  
67 bioavailable Si has become an issue especially for cultivated soils naturally or anthropically  
68 depleted in plant available Si (Tubana et al. 2016; Haynes, 2017). The characterization of  
69 bioavailable soil Si is still empirical and the knowledge of fundamental mechanisms that drive  
70 the biogeochemical cycle of silica under cultivation are necessary for a better assessment of  
71 the impact of Si on plant development (Cooke and Leishman, 2016) as well as the future  
72 impact of global change on the Si cycle (Schaller et al., 2021; Yang et al., 2019, 2020).

73 There are several main reservoirs of Si in soils that can be used by plants provided that  
74 the Si leaching from these solid phases to the interstitial porewater is fast enough. First, these  
75 are primary and secondary crystalline silicate minerals that constitute the bulk of bottom and  
76 intermediate soil horizons. The reactivities (dissolution rates) of most Si-bearing primary and  
77 secondary aluminosilicate minerals commonly present in soils and quartz are quite low (Schott  
78 et al., 2019) and not capable of providing sufficient amount of labile Si required for plant

79 growth, especially when the state of weathering is well advanced (de Tombeur et al., 2020).  
80 Possible exceptions are soils developed on highly reactive materials such as volcanic ash  
81 (Ugolini and Dahlgren, 2002; Vandekerkhove et al., 2016) or wollastonite (Cho et al., 2010).  
82 Amorphous materials, including biogenic silica (mainly phytoliths) and short-range order  
83 minerals have been identified as another potential source of dissolved Si (Puppe, 2015;  
84 Meunier et al., 2017; Cornu et al., 2022; Li et al., 2022). The reactivity of plant phytoliths is  
85 quite high, greatly exceeding that of clay minerals (Frayse et al., 2009). The uptake of Si  
86 from phytoliths allows the plants to overcome labile Si deficit as it is established in various  
87 cultivated and pristine environments (Desplanques et al., 2005; De Tombeur et al., 2020;  
88 Gérard et al., 2008). Finally, the plant litter itself, where Si is present as both phytoliths and  
89 the dispersed form (Watteau and Villemin, 2001; Watteau et al., 2002; Fraysse et al., 2010),  
90 and Si which is bound to organic compounds (Kolesnikov and Gins, 2001), including humic  
91 acid-Al-Si complexes (Merdy et al., 2022) represent another potentially labile pool of Si for  
92 plants. For example, in the Amazonian forest, the Si input from the litterfall on top of the soil  
93 is about four times greater than the Si leached out of the system (Lucas et al., 1993).

94 In most soils, the Si pool available for plants may comprise all the reservoirs listed  
95 above. In addition, some Si can be adsorbed on the surfaces of soil minerals and organic debris  
96 and thus can be easily mobilized to aqueous solution (Rückert, 1992; Brinkman, 1970).  
97 However, aggregates in the soils may slow the process of dissolved Si mobilization (Li et al.,  
98 2022). So far, plant available Si (PAS) has been empirically estimated by chemical procedures  
99 using extractants such as 0.01 CaCl<sub>2</sub> (i.e., Haysom and Chapman, 1975) that provide a positive  
100 correlation with plant yield (Babu et al., 2016; Narayanaswamy and Prakash 2010). Various  
101 PAS quantification methods demonstrated positive correlations with factors that may affect Si  
102 availability, such as pedological and geological conditions (Landré et al., 2020), soil pH  
103 (Meunier et al., 2018; Caubet et al., 2020; Schaller et al., 2021), weathering stage (Klotzbücher

104 et al., 2014) and the presence of phytoliths (De Tombeur et al., 2020) and clay fraction and  
105 short-range ordered (SRO) aluminosilicates (e.g. allophanes and imogolites; Caubet et al.,  
106 2020; Cornu et al., 2022; Keller et al., 2021). Cornu et al (2022) found that PAS based on the  
107  $\text{CaCl}_2$  method was generally higher in cultivated soils than in forest soil and was controlled by  
108 pH and the presence of allophanes. However, the PAS methods do not allow to propose general  
109 laws of Si release rate. For this, laboratory experimental approaches are needed. Thus, Barao et  
110 al. (2019) used kinetic batch experiments with Belgium soils and found that reactivity of Si in  
111 croplands were higher than that of forest and pasture soils. Ronchi et al. (2015) used a leaching  
112 test approach on soil column to evaluate the dissolution rate of Si and to compare it with that of  
113 single soil minerals and biogenic Si pools. They found that the Si release from Belgian  
114 Luvisols and Sweden Cambisols are controlled by pH and decline from forest to cropland while  
115 PAS ( $\text{CaCl}_2$  method) showed an opposite trend. Accordingly, more data is required to  
116 disentangle the significance of rate dissolution laws in soils and the impact on cultivated lands.

117 Building on this information, the purposes of this study are twofold. First, we aimed at  
118 assessing the rates of Si release from French temperate soils developed from calcareous or  
119 loess parent materials (characterized by Cornu et al., 2022), collected in adjacent cultivated and  
120 forest plots. Specifically, we intended to quantify the impact of solution composition (pH,  
121 presence of organic ligand or bicarbonate ion) on Si release rate in dynamic experiment and to  
122 compare Si release rate from various soils to that of clay minerals and Si-bearing amorphous  
123 compounds. Secondly, we focused on measuring initial, non-stationary Si release from soil,  
124 allowing to quantify the pool of most labile soil Si in order to relate it to conventionally-  
125 measured forms of Si in soils. In this regard, the present work is devoted to identify the  
126 physico-chemical (abiotic) factors controlling dynamic Si pool in soil. Furthermore, it allows  
127 quantifying possible bioavailable pool, rather than characterizing real bioavailability of silicon.

128 For the latter, specially designed mesocosm-level experiments with Si uptake by live plants and  
129 analysis of Si concentration in the biomass are necessary.

130

131

## 132 **2. Materials and Methods**

133 We have chosen seven French soils developed in calcareous or loess parent material in  
134 the temperate climate zone: 2 hypereutric cambisols (called ‘calcisol’ for brevity), 2 calcaric  
135 cambisols (‘calcosol’), 2 luvisols, and 1 albeluvisol (WRB, 2006 soil classification;  
136 Chesworth et al., 2008). Their basic physical and chemical properties are listed in **Table 1** and  
137 more information is provided in Cornu et al. (2022). We used a paired site approach which  
138 includes adjacent soils with identical pedological factors (topography, parent material, climate  
139 and age) but different in their land use (cultivated versus forest soils). Localization of sampled  
140 soils is illustrated in Supplementary **Figure S1**. The soils were air dried, sieved through 2 mm  
141 sieve and sterilized prior to using for dissolution experiments. Specific surface area was  
142 measured using multiple point N<sub>2</sub> adsorption (Micrometrics ASAP 2010 apparatus) after  
143 degassing during 48 h at 120°C.

144 The experimental setup involved two independent dynamic (flow-through) reactors,  
145 operating at high and low ratio of fluid to soil (**Fig. 1**). In order to measure Si release rate  
146 from soils as a function of solution pH, at high fluid : solid ratio, we used classic mixed-flow  
147 reactor (**Fig. 1 A**), developed for measuring the dissolution rates of individual minerals (i.e.,  
148 Pokrovsky et al., 2009, 2021; Schott et al., 2009). Similar reactors were used for assessing the  
149 Si-based reactivity of soil clay minerals (i.e., Köhler et al., 2003, 2005; Golubev et al., 2006),  
150 plant phytoliths (Frayse et al., 2008, 2009) and whole plant litter (Frayse et al., 2010). These  
151 reactors allow measuring steady-state Si release rate at fixed pH and other solution  
152 parameters. Steady-state dissolution rates were obtained at distinct solution compositions and

153 pH at a constant temperature of  $25.0 \pm 1.0^\circ\text{C}$  in a thermostated room. Reacting fluids were  
154 comprised of deionized degassed  $\text{H}_2\text{O}$ , Merck reagent grade  $\text{HCl}$ ,  $\text{NaOH}$ ,  $\text{NaHCO}_3$ ,  
155  $\text{NaCH}_3\text{COO}$ , and  $\text{NaCl}$ . All solutions were prepared from  $18 \text{ M}\Omega$  ultrapure sterile water  
156 (MilliQ Plus system) having a blank of dissolved organic carbon  $< 0.05 \text{ ppm}$ . The input fluid  
157 was stored in a polyethylene container protected against  $\text{CO}_2$  uptake from the atmosphere. It  
158 was injected into the reaction vessel using a Gilson® peristaltic pump at typical flow rates  
159  $0.1 \text{ mL min}^{-1}$ . The reactor consisted of a  $25 \text{ mL}$  Teflon vessel which was continuously stirred  
160 with a floating Teflon supported magnetic stirrer, which prevented soil grinding during  
161 experiments. The reactive solution left the reactor through a series of  $2.5 \text{ }\mu\text{m}$  polycarbonate  
162 and  $0.45 \text{ }\mu\text{m}$  Nylon filters mounted in a row. All reactors initially contained  $1.50 \text{ g}$  of soil.  
163 The experiments started from injecting into reactor the Milli-Q water at  $\text{pH} = 5.6$ , followed by  
164 a mixture of  $10 \text{ mM NaCl}$  and  $1 \text{ mM NaHCO}_3$  at  $\text{pH} = 8$ , and a mixture of  $5 \text{ mM NaCl}$  and  $5$   
165  $\text{mM Acetic acid}$  at  $\text{pH} = 4.2$ . The duration of each run ranged from  $200$  to  $500 \text{ h}$ . Finally, the  
166 reactor was run again with Milli-Q at  $\text{pH}$  around  $6$  during  $450 \text{ h}$ . For most experiments lasting  
167  $40\text{-}60$  days in total, one sampling per day was performed. The total mass of soil in the reactor  
168 was measured at the beginning and at the end of experiment; no sizable changes (i.e., within  
169  $10 \%$ ) have been detected.

170 Steady-state dissolution rates ( $R_{Si}$ ,  $\text{mol g}_{\text{soil}}^{-1} \text{ d}^{-1}$ ) were computed from measured  
171 solution composition using Eqn. 1:

$$172 \quad R_{Si} = -q \cdot [\text{Si}(\text{aq})]_{\text{outlet}} / m \quad (1)$$

173 where  $q$  ( $\text{L s}^{-1}$ ) designates the fluid flow rate,  $[\text{Si}(\text{aq})]_{\text{outlet}}$  ( $\text{mol L}^{-1}$ ) stands for the outlet Si  
174 concentration (M), and  $m$  (g) refers to the total soil mass of soil present in the reactor,  
175 respectively. Uncertainties on the steady-state rate constants are dominated by the uncertainty  
176 on the standard deviation on average Si a concentration at the steady-state ( $\pm 10\text{-}20 \%$ ).



177           The second type of approach involved flow-through column experiments used for  
178 evaluating water-labile pool Si in soils (**Fig. 1 B**). Similar column experiments were shown to  
179 be efficient for measuring flux of Si from soils and assessing Si release rate at close to  
180 equilibrium conditions, at high soil : fluid ratio, most pertinent to natural settings (Ronchi et  
181 al., 2015). This setup involved small polypropylene column (diameter 1 cm, length 5 cm)  
182 packed with sieved (< 2 mm) soils. The column was filled with 1 g of upper 0-10 cm horizon  
183 of forest soil (F1) and 3 g of lower 20-30 cm horizon of forest soils (F2); we used hypereutric  
184 cambisol, calcareic cambisol and luvisol for these experiments. Fine soil sample (< 2 mm) was  
185 placed on the top of Teflon cotton supported by a porous (< 500  $\mu\text{m}$ ) Teflon disk; the outlet of  
186 the column was fitted with a 0.45  $\mu\text{m}$  filter, and the fluid flow direction was from the bottom  
187 to the top. Similar to mixed-flow reactors, three inlet solutions were used in column  
188 experiments: Milli-Q water at pH = 5.6, a mixture of 10 mM NaCl and 1 mM NaHCO<sub>3</sub> at pH  
189 = 8, and a mixture of 5 mM NaCl and 5 mM Acetic acid at pH = 4.2. Continuous  
190 breakthrough curves of solutes were monitored from specific conductivity and pH  
191 measurements of the outlet fluid. These allowed integrating the amount of Si released from  
192 soil column as a function of time and over full duration of experiments. Similar approach for  
193 identifying the labile Si pool was used in batch experiments of other studies (e.g., Barao et al.  
194 2019). Because the concentration of Si in the column outlet solution strongly decreased over  
195 the first 10-100 h to some steady-state concentrations (see section 3.2 below), while the pH  
196 was buffered by acetate or carbonate buffer, the labile (fast leachable) pool of Si in soil  
197 sample was calculated for discrete time interval (0-10 h and 10 – 100 h). For this, we  
198 numerically integrated the amount of released Si with 1 to 2 h step for the 0-10 h period and  
199 with 10 to 20 h step for the 10-100 h period and normalized the mass of released Si to the  
200 total amount of soil in the column.

201 The pH in the outlet solution was measured using a combination glass electrode  
202 (Mettler Toledo) calibrated with NIST buffers (pH 4.01, 6.865, 9.18 at 25°C), with an  
203 uncertainty of  $\pm 0.01$  units. Aqueous silica concentration was determined using Quadripole  
204 ICP MS Agilent 7500 ce, with an uncertainty of 2% and a detection limit of  $3.6 \cdot 10^{-7}$  M. The  
205 quality of measurements was monitored by regular analysis of SLRS-5 certified sample (2.2  
206 mg L<sup>-1</sup> Si) and an in-house standard of 0.01 M NaCl with ten times lower Si concentration.

207 Statistical treatment of the data included mean values and their standard deviations (in  
208 case of replicates and for calculating the steady-state concentrations from 4 to 5 sampling  
209 points) and linear regressions. Pairwise (Pearson) correlations were used to assess the  
210 relationship between various forms of Si in soils as measured by standard techniques (e.g.,  
211 Cornu et al., 2022) and the labile Si pool measured in the experiments. Further, a pairwise  
212 comparative analysis was run via non-parametric Mann-Whitney test (U-test) to detect the  
213 differences between Si release rate or Si pools in datasets of different soils. The level of  
214 significance was fixed at 0.05 (95% confidence level) to consider a result as statistically  
215 notable. All plots were built using MS Excel 2016 and the Statistica-12 software package  
216 (<http://www.statsoft.com>).

217

218

### 219 **3. RESULTS**

#### 220 *3.1. Long-term dissolution in mixed-flow (open) reactors*

221 Results of 16 long-term (10 - 15 days each) soil dissolution experiments are listed in  
222 Table 2 and illustrated in **Fig. 2** for two forest and two agricultural soils. The steady state  
223 outlet Si concentrations were typically achieved after first 20 h corresponding to 5 residence  
224 times of the fluid in the reactor. In this regard, the chemical and mechanical steady-state were  
225 similar. The outlet Si concentration responded to the change of chemical composition and the

226 pH of the inlet fluid. Silica concentration increased in the order “Milli-Q (pH = 6.0 - 6.5) <  
227 0.01 M NaCl/NaHCO<sub>3</sub> (pH = 8.0±0.2) < 0.01 M Na Acetate (pH = 4.2±0.1)”. After 800 h of  
228 experiment, we injected again the MilliQ water, and in most cases, the outlet concentration of  
229 Si were within ±20-30% of the values obtained at the beginning of experiment.

230 The Si release rates ( $R_{Si}$ ) calculated from steady-state outlet Si concentration (Eqn. 1)  
231 presented a weak dependence on solution pH which was, however, depended on the type of  
232 soils (**Fig. 3**). The hypereutric cambisol  $R_{Si}$  decreased by a factor of 1.6 when pH increased  
233 from 4.2 to 6.5, had a minimum at pH 6.5 and then stabilized at pH close to 8 (**Fig. 3 A**). The  
234 calcaric cambisol  $R_{Si}$  decreased by a factor of 2±0.5 from pH 4.2 to 7-8 (**Fig. 3 B**). The luvisol  
235  $R_{Si}$  exhibited a minimum at pH around 6 (**Fig. 3 C**). Finally, the albeluvisol stood apart from  
236 all other soils and yielded a 2-fold increase in  $R_{Si}$  when the pH increased from 4.1 to 8.2 (**Fig.**  
237 **3 D**). None of the studied soil yielded significant (Mann-Whitney test,  $p < 0.05$ ) difference in  
238 Si release rate between forested and cultivated soils. The plot of all soils in log  $R_{Si}$  scale  
239 demonstrated overall weak dependence on pH (**Fig. 4**). When normalized to specific surface  
240 areas, the rates of Si release from various soils exhibited the order ‘hypereutric cambisol <  
241 luvisol < calcaric cambisol ~ albeluvisol’ (**Table 2; Fig. S2** of the Supplement).

242

243

### 244 *3.2. Silicon leaching from soils in the column reactor experiments*

245 The rates of Si release from forest soils were calculated from the Si concentration at  
246 steady-state (typically after 10-100 h of reaction) in the column experiments using Eqn. 1.  
247 The rates measured in column reactors are listed in **Table 3**. The rates ranged from  $1.0 \times 10^{-6}$   
248 to  $1.9 \times 10^{-7}$  mol Si g<sup>-1</sup> day<sup>-1</sup> for 800 to 150 µg L<sup>-1</sup> of dissolved Si output concentration. These  
249 values are fairly comparable with  $R_{Si}$  measured in mixed-flow reactors, when the ratio soil :  
250 fluid was one order of magnitude higher.

251 At the same time, the initial outlet Si concentrations over first 4 hours were very high,  
252 ranging from 4000 to 8000  $\mu\text{g L}^{-1}$  (**Fig. 5**). Specifically, the outlet Si concentrations decreased  
253 from 6000 to 1000  $\mu\text{g L}^{-1}$  over 10 h reaction with hypereutric cambisols, from 4000 to 1000  
254  $\mu\text{g L}^{-1}$  over 7 h for calcaric cambisol and from 8000 to 500  $\mu\text{g L}^{-1}$  over 6 h with luvisol. The  
255 initial outlet Si concentrations corresponded to instantaneous, non-steady state  $R_{Si}$  around  $10^{-5}$   
256  $\text{mol Si g}^{-1} \text{ day}^{-1}$ . This is an order of magnitude higher than the rates at the steady state  
257 measured in both mixed-flow reactor and column experiments. The numerical integration of  
258 the breakthrough curve (i.e., Si concentration vs time over first 0-10 h of reaction) in the  
259 Milli-Q water allowed quantifying the pools of labile Si, equaled to  $0.08 \pm 0.01 \text{ mg Si g soil}^{-1}$   
260 for hypereutric cambisols and  $0.040 \pm 0.002 \text{ mg Si g soil}^{-1}$  for luvisols. These numbers were  
261 calculated from the average of two samples for each soil (1166 (F1+F2) and BS2 (F1+F2) of  
262 hypereutric cambisol; 340 (F1+F2) and 62 (F1+F2) of luvisol). The calcaric cambisols  
263 demonstrated much longer tail of high outlet concentrations, persistent over 90 h of reaction;  
264 the overall labile Si for calcosol 755 F1 is estimated as  $0.145 \pm 0.02 \text{ mg Si g soil}^{-1}$ , although  
265 the actual uncertainties may be much higher. This particular behavior of calcosol could be  
266 linked to progressively dissolving carbonate mineral grains that buffered the release of Si  
267 from relevant silicate pools.

268 For calcaric cambisol and hypereutric cambisol, approximately half of the labile pool  
269 was mobilized over first 0-10 h of reaction (**Table 4**). In contrast, > 90 % of labile Si pool in  
270 the luvisol was released over first 4 h of reaction or even faster, given insufficient temporal  
271 resolution at the beginning of experiments. This difference can be tentatively linked to the  
272 fact that the cambisol had much higher quantity of clay minerals compared to the luvisol.

273

274 *3.3. Testing the link between experimental Si release rate, labile Si pool and analytical*  
275 *Si pools in soils*

276 Based on recent study of various conventional analytical pools of Si in soils (Cornu et  
277 al., 2022, see their **Table 1**), we tested a correlation of these pools with experimentally  
278 measured Si release rates in mixed flow reactors and labile Si pools measured in the column  
279 experiments. For this, we used steady-state  $R_{Si}$  values from mixed-flow (**Table 2**) and flow-  
280 through column (**Table 3**) experiments, and pools of labile soil Si integrated over 0-10 and  
281 10-100 h of reaction in column experiments at various pH (**Table 4**). In the latter case, the  
282 reason for considering independently these two time intervals is that they could correspond to  
283 two pools of leachable Si, as seen from the relevant breakthrough curves (**Fig. 5**). In contrast,  
284 after 100 h of reaction, there are steady-state Si release processes that can be better reflected  
285 by a stationary Si release rate ( $R_{Si}$ ). There was no significant (at  $p < 0.05$ ) correlation between  
286 Si release rate neither in mixed flow nor column reactor, and any conventional analytical  
287 forms of soil Si, including content of total Si, oxalate-,  $\text{CaCl}_2$ -, and dithionite-extracted Si and  
288 phytoliths in studied soils (**Table S1** and **Fig. S3** of the Supplement). However, the pools of  
289 labile Si quantified from column experiments on forest soils exhibited significant correlations  
290 ( $p < 0.05$ ) with certain labile Si forms in soils (**Table 5**). The strongest correlations ( $R^2 =$   
291  $0.94-0.98$ ,  $p < 0.01$ ) were observed between Si pool mobilized over 10-100 h reaction in the  
292 Milli-Q water or over 0-10 h in the acetate buffer and Si concentration in the form of  
293 allophanes/imogolites as extracted by Tamm method ( $\text{Si}_O$ ), which provides amorphous Fe/Al  
294 compounds (**Fig. 6 A, B**). The pool of labile Si released over 10-100 h in the acetate buffer  
295 strongly ( $R^2 = 0.97$ ,  $p < 0.01$ ) correlated with  $\text{Si}_{\text{CaCl}_2}$  forms in soils (soluble, bioavailable Si  
296 extracted with  $\text{CaCl}_2$ ), **Fig. 6 C**. Note that the correlations of different Si forms in soils  
297 determined in Cornu et al. (2022) with total (0-100 h) leachable pool of Si determined in  
298 column experiments were much lower than those for two fractional pools (0-10 and 10-100  
299 h). The total chemical pool of Si in soils ( $\text{Si}_{\text{tot}}$ ) strongly ( $R^2 \geq 0.94$ ,  $p < 0.01$ ) anti-correlated

300 with both acetate- and Milli-Q reacting pools determined in column experiments (**Fig. S4** of  
301 the Supplement).

302

303

304

## 305 **4. DISCUSSION**

### 306 *4.1. Comparison of Si release rate between bulk soil, minerals, and phytoliths*

307 A comparison of whole soil Si release rates with dissolution rates of common soil  
308 minerals and plant phytoliths measured in the mixed-flow reactor similar to the one used in  
309 this study is given in **Figure 4**. Added to this figure also the recent data for allophane  
310 dissolution in batch reactors (Ralston et al., 2018) and results of column leaching experiments  
311 on forest soils (Ronchi et al., 2015). Noteworthy that all soils except albeluvisol at pH 4.2  
312 exhibited sizably higher (1-2 orders of magnitude)  $R_{Si}$  values compared to those of typical  
313 clay minerals present in soil. Whilst in acidic environment (pH = 4.0-4.5), the rates of Si  
314 release from the whole soil are 2 to 10 times higher than those of soil clay minerals, at pH = 6  
315 to 8.5 the difference sizably increases because the clay minerals decrease their rates with pH  
316 between  $4 < \text{pH} < 7.5$ . At the same time, this trend of  $R_{Si}$  with pH qualitatively corresponds to  
317 that observed for luvisols and hypereutric cambisols (calcisol) in **Fig. 3**. In contrast, the  $R_{Si}$  of  
318 French soils developed in calcareous or loess parent material stay essentially constant at  $(10 \pm$   
319  $5) \times 10^{-6}$  mol Si /g<sub>soil</sub>/day, or  $(8 \pm 3) \times 10^{-8}$  mol Si /m<sup>2</sup><sub>soil</sub>/day. The calcaric cambisol (calcosol)  
320 and albeluvisol exhibited a different trend of  $R_{Si}$  with pH (Fig. 3). The dissolution rate of  
321 albeluvisol increases with pH, which is also observed for quartz given the importance of the  
322 quartz fraction in this type of soil, including the  $< 2 \mu\text{m}$  fraction (i.e., 60 % of the crystalline  
323 silicates, Cornu et al., 2022). However, the mass-normalized Si release rate from quartz is  
324 several orders of magnitude lower than that from studied soils, and the slope of  $\log R_{Si} - \text{pH}$

325 dependence for quartz is much higher than that observed for albulivisol (factor of 2 and 0.5  
326 per one pH unit, respectively). Furthermore, the luvisol also contains sizable amount of quartz  
327 but did not yield an increase in  $R_{Si}$  with pH. For the calcareic cambisols (calcosol), there is a  
328 constant decrease of the dissolution rate with the pH. This could be due to a dissolution of the  
329 carbonate fraction in the first stage of the experiment.

330 Overall, at pH around 7-8, the difference in Si release rate between typical soil clay  
331 minerals and whole soils reaches more than 1.5-2.0 orders of magnitude. This is rather  
332 unexpected result, given that the synthetic clays (kaolinite, illite, chlorite and smectite) used  
333 for this plot constitute the majority of soils studied in this work (e.g., Cornu et al., 2022).  
334 However, one should be careful when performing such a comparison: individual clays used in  
335 previous experiments are generally better crystalline and larger than those encountered in  
336 soils. As a result, the mass-normalized reactivity of natural soil clays may be higher than  
337 those of synthetic crystalline minerals, as also demonstrated in some mineral bag natural  
338 experiments (e.g., Cornu et al., 1995).

339 The Si release rates from the whole soil measured in this study are drastically different  
340 from those of plant phytoliths as also shown in **Fig. 4**. Not only the plant phytoliths are 1 to 3  
341 orders of magnitude more 'reactive' than soils (Fraysse et al., 2009), but the shapes of  $\log R_{Si}$   
342 - pH dependences between soils and phytoliths are totally different. Taken together, negligible  
343 role of phytoliths in Si supply to aqueous solution in experimental reactors and column-  
344 through experiments of the present study is demonstrated by lack of correlations (or negative  
345 correlations) between the labile Si pool and phytoliths content in forest soils (**Table 5**), and  
346 totally different pattern of rate dependence on solution pH for studied soils and plant  
347 phytoliths (**Fig. 4**). As such, the reactivity of Si in soils investigated in this study cannot be  
348 explained by a presence of small fraction of highly reactive phytoliths. In contrast to  
349 phytoliths, the plant litter exhibits quite weak dependence of  $R_{Si}$  on pH; for 6 various plants,

350 the Si release rate ranged from  $10^{-7}$  to  $10^{-5}$  mol  $g_{\text{plant}}^{-1} d^{-1}$  with very weak increase in  $R_{Si}$  with  
351 pH increase (ca., 0.3 log  $R$  unit per 5 pH unit, Fraysse et al., 2010). However, it is very  
352 unlikely that the presence of small (1-10%) amount of fresh, Si-rich plant litter in studied soils  
353 can explain their reactivity in aqueous solution: the content of refractory organic matter in  
354 soils is too low and highly variable among soils (10 to 70 g  $kg^{-1}$ , see **Table 1**) to allow a  
355 realistic impact of admixture of plant litter/soil humic material as a source of Si in aqueous  
356 solution contacting with soil in our experiments.

357 To get further insights into mechanisms driving Si release from soils in our  
358 experiments, we consider several possible pools of Si. First, in addition to poorly reactive  
359 quartz, these are ‘primary’ crystalline clays (kaolinite, illite, chlorite) and secondary, poorly  
360 crystalline smectites and/or interlayered illite-smectite minerals (Cornu et al., 2022). Second,  
361 there are amorphous/poorly crystalline imogolites and allophanes, including organo-alumino-  
362 siliceous, organo-Fe-Al-siliceous compounds (Farmer et al., 1980; Matichenkov and Snyder,  
363 1996; Ralston et al., 2021). While the dissolution of ‘usual’ clays cannot provide the observed  
364 magnitude and pH-dependent pattern of  $R_{Si}$ , the reactivity of amorphous Si-bearing mineral  
365 and organo-mineral compounds such as pure end-member allophanes, including both Fe-free  
366 and Fe-rich compounds (i.e., Ralston et al., 2021) is an order of magnitude higher than that of  
367 soils studied in this work (see **Fig. 4**) and thus allophane cannot be excluded as a source of Si  
368 released from soils. An indirect evidence of the importance of this pool of soil Si in the short-  
369 term Si release patterns in our experiments is strong positive correlation observed between the  
370 labile Si assessed in column filtrations and  $Si_O$  measured by Tamm extraction procedure, and  
371 Si extractable by  $CaCl_2$  (**Table 5, Fig. 6**). This is consistent with a similarity of the  $R_{Si} - pH$   
372 dependence between allophanes and the calcaric cambisol, the soil in which allophane are the  
373 most present.



374 It has been known for long that silicic acid is readily adsorbed by and released from  
375 soils and soil minerals (Beckwirth and Reeve, 1963, 1964; McKeague and Cline, 1963;  
376 Haynes and Zhou, 2020). Therefore, the third major pool of soil Si is siliceous acid and  
377 silicate ions, adsorbed onto surfaces of soil minerals, first of all Al and Fe oxyhydroxides  
378 (Bruun Hansen et al., 1994; Hingston and Raupach, 1967). In particular, strong adsorption of  
379 Si onto Fe(OH)<sub>3</sub> is fairly well known (Dietzel et al., 2002; Vempati and Loeppert., 1989). The  
380 adsorption/desorption rate of silica from solid surfaces is usually very fast, and the  
381 equilibrium is established over the order of first hours (Beckwirth and Reeve, 1963, 1964).  
382 The majority of Si adsorbed on the surface of ferrihydrite and goethite at room temperature  
383 occurred over first 50 to 100 h (Delstanche et al., 2009). As such, the initial high Si  
384 concentration in flow-through column experiment can stem from mobilization of adsorbed Si  
385 pool. Consistent with this possibility is the observation that the reversible adsorption (and,  
386 consequently, desorption) of silicic acid onto/from Fe hydroxide is independent on pH at  $5 \leq$   
387  $\text{pH} \leq 8$  (Sigg and Stumm, 1981).

388 Finally, a sizable pool of Si in soils may be represented by biogenic silica such as  
389 phytoliths, diatom frustules and exo-skeletons of protozoae (Sommer et al., 2006). The  
390 dissolution of this bulk biogenic silica, however, cannot provide the observed pH-independent  
391 pattern of Si release from soils studied in this work. In contrast to 'classic' phytolith such as  
392 those investigated by Fraysse et al (2006, 2009), small size phytogenic silica ( $< 5 \mu\text{m}$ , by  
393 definition proposed in Sommer et al., 2006) has not been investigated from the view point of  
394 its reactivity in aqueous solution. However, it is unlikely that both the magnitude and pH-  
395 dependence of small size phytogenic  $R_{Si}$  would be different from those of phytoliths: the grain  
396 size has no sizable impact on surface-normalized mineral dissolution rates, unless these  
397 minerals were subjected to strong shock which can generate dislocations (e.g., Schott et al.,  
398 2009). The same is true for abiotically formed amorphous silica which is known to precipitate

399 from soil solution in the form of pure phases on mineral surfaces (Drees et al., 1989): the  
400 strongly pH-dependent pattern of amorphous silica dissolution rate is different from much  
401 weaker pH dependence or even pH-independent pattern of Si release from soils, studied in  
402 this work.

403 We observe a sizable, about two orders of magnitude, difference in Si release rate  
404 measured for the French soils in the mixed-flow reactor in this study and the rates of Si  
405 leaching in column experiments with forest and arable Swedish cambisols and Belgian  
406 luvisols reported by Ronchi et al. (2015), **Fig. 4**. We tentatively explain this difference by  
407 first, more important role of allophanes and less important role of clay minerals in controlling  
408 Si release from studied soils compared to cambisols and luvisols of Ronchi et al. (2015). Note  
409 that, although the rates of Si release from luvisol and hypereutric cambisol decrease with pH  
410 similar to that of Ronchi et al. (2015), the  $R_{Si}$  measured in this study are  $2.0 \pm 0.5$  orders of  
411 magnitude higher. Second, a lack of pH-dependence for Si release rate from soils in this study  
412 (notably of calcaric cambisol and albeluvisol) and similarity of Si release rate in Ronchi et al  
413 (2015) with common soil clays suggest the dominance of different mineral pools determining  
414 the Si release pattern. In particular, we noted an order of magnitude higher  $Si_{oxalate}$  content in  
415 the soils of this study compared to those of Ronchi et al. (2015). Moreover, the initial outlet Si  
416 concentration in experiments of Ronchi et al. (2015) was  $> 10$  times higher than that in the  
417 present study and it achieved 50 to 70 mg L<sup>-1</sup>. At such high concentrations, the Si release  
418 becomes limited by solubility of amorphous silica ( $SiO_2 \times nH_2O$ ). It is thus possible that  
419 mixed-flow reactors with high fluid:solid ratio, used in this study and the column reactors  
420 with very low fluid:solid ratio of Ronchi et al (2015) do not probe the same pools of soil Si,  
421 despite similar time scale used to extract the steady-state rates. Another possible explanation  
422 could be linked to different nature and relative abundances of crystalline clays and short range  
423 ordered minerals in soils used by these two studies.

424

425 *4.2. Si release from soils in natural settings*

426       Regardless of exact chemical and mineralogical nature of leachable Si pool in the  
427 studied soils, the main consequence of the presence of this labile Si is that it can be quickly,  
428 on the order of hours or even minutes, mobilized into aqueous solution (i.e., after rain  
429 infiltration) and become available for plant uptake. Overall, the pool of fast (0-10 and 10-100  
430 h) water-leachable, mobile Si in forest soil ranges, depending on pH, from 0.04 mg Si g<sub>soil</sub><sup>-1</sup>  
431 for luvisol to 0.08 mg Si g<sub>soil</sub><sup>-1</sup> for hypereutric cambisol and calcareous cambisol (**Table 4**).  
432 Assuming that only upper 0-20 cm layer of soil reacts with aqueous solution (**Table 2**), and  
433 considering typical soil stock (0-20 cm) of 2×10<sup>6</sup> kg ha<sup>-1</sup> (Winfried et al., 2018), this gives the  
434 labile Si stock of 80 to 160 kg bioavailable Si ha<sup>-1</sup>. This value can meet the annual (or even  
435 monthly) requirements of plants in bioavailable Si (2 to 90 kg Si ha<sup>-1</sup>, Cornelis et al., 2011;  
436 Cornelis and Delvaux, 2016). In the temperate forest, Si uptake flux by deciduous trees and  
437 Douglas fir ranges from 36 to 46 kg ha<sup>-1</sup> y<sup>-1</sup>, and that of the pine forest does not exceed 7 kg  
438 ha<sup>-1</sup> y<sup>-1</sup> (Lucas, 2001; Gérard et al., 2008). Therefore, experimentally measured mobile Si pool  
439 in forest soils is potentially capable of providing the totality of this demand; however, more  
440 measurements on specific soils are needed to further quantify this potential.

441       The upper (0-20 cm) soil profile can be considered as a mixed-flow reactor with  
442 rainwater input corresponding to annual precipitation minus evapotranspiration, or runoff of  
443 the riverine watershed. Combined with the mass of soil and the rates of labile Si release from  
444 bulk soil to the outlet river water, this allows determining the concentration  $C_{Si}$ :

445 
$$C_{Si} = R_{Si} \times m / D \quad (2)$$

446 where  $m$  is the mass of soil in the ecosystem (kg ha<sup>-1</sup>),  $D$  is the flow rate or annual runoff  
447 (precipitation minus evapotranspiration), in mm yr<sup>-1</sup> or L ha<sup>-1</sup>, and  $R_{Si}$  is the experimental  
448 dissolution rate (mol<sub>Si</sub> g<sub>soil</sub><sup>-1</sup> d<sup>-1</sup>). To calculate  $C_{Si}$ , we will assume typical parameters of

449 temperate forest at the steady-state with respect to biomass growth and decay:  $m_{0-20\text{ cm}} = 200$   
450  $\text{kg m}^{-2}$  or  $2 \times 10^6 \text{ kg ha}^{-1}$  (Winfried et al., 2018),  $D = 13700 \text{ L d}^{-1} \text{ ha}^{-1}$  corresponding to a runoff  
451 of  $500 \text{ mm y}^{-1}$ , and  $R_{\text{Si}} = 10^{-6} \text{ mol Si g}_{\text{soil}}^{-1} \text{ d}^{-1}$  corresponding to Si release rate from soil in  
452 circumneutral solutions (pH = 5-8) measured in this study, see **Table 2** and **Fig. 4**. This yields  
453  $C_{\text{Si}} = 0.15 \text{ mol L}^{-1}$  or  $4100 \text{ mg Si L}^{-1}$ , which is several orders of magnitude higher than typical  
454 Si concentration in surface waters (4.2-5.0  $\text{mg L}^{-1}$ , Gaillardet et al., 1999) and interstitial soil  
455 solutions of surficial horizons (2.8 – 14  $\text{mg L}^{-1}$ , Sommer et al., 2006; Pokrovsky et al., 2005a,  
456 b). Therefore, less than 1% of upper soil, receiving the incoming rainwater and releasing Si at  
457 the steady-state conditions (i.e., no aggrading forest and no silica precipitation in deeper parts  
458 of the soil profile) is capable to provide the observed Si concentration in surface waters.

459 An unexpected result of this study is rather similar values of Si release rate regardless  
460 of soil type, agricultural use, and solution pH. Note that we could not use coupled forest-  
461 cultivable soil approach for quartz-rich and clay-poor sand dunes because agricultural soils  
462 were not available for such substrates. It is thus possible that ‘universal’ Si release rate  
463 proposed in this study might turn out to be not so ‘universal’ if screened across all possible  
464 soils, including clay-poor sands or ultisols (red clay soils), which are dominated by 1:1 clay  
465 minerals instead of 2:1 clays studied in this work. Therefore, keeping in mind that the  
466 substrates investigated in this work are only representative for well differentiated soil  
467 developed on loess and poorly differentiated soil developed on calcareous soils, we can  
468 extend the discussion to more general case of various lithological context. We note that the  
469 natural Si export fluxes (yields) by rivers from watersheds are also similar (by an order of  
470 magnitude), despite large variations in soil type, rock lithology, vegetation, runoff and soil  
471 solution pH across different biomes as illustrated below. Thus, the total annual Si export  
472 fluxes by rivers of boreal and temperate watersheds, although sizably dependent on runoff,  
473 are within the same order of magnitude regardless of climate and lithological context (basalts,

474 granites, sedimentary rocks and even peatland environments). For example, in boreal and  
475 temperate zone, riverine Si yield ranges from 0.3 to 3.0 t Si km<sup>2</sup> y<sup>-1</sup> (Oliva et al., 2003;  
476 Zakharova et al., 2005, 2007; Pokrovsky et al., 2005b, 2020; Chupakov et al., 2020). A recent  
477 study of 20 Canadian rivers of contrasting land cover, lithology, soil type and climate  
478 demonstrated a range of Si export fluxes from 0.2 to 6.6 t km<sup>2</sup> y<sup>-1</sup> with an average value of  
479 1.6 t km<sup>2</sup> y<sup>-1</sup> (Phillips and Cowling, 2019). Even in fresh Hawaiian basalts, the range of Si  
480 export rate is only from 0.4 to 15 t km<sup>2</sup> y<sup>-1</sup> (Derry et al., 2005), similar to silica export fluxes  
481 from the rooting zone (20–30 cm depth) in these tropical settings (1.1 to 25 t km<sup>2</sup> y<sup>-1</sup>, Hedin  
482 et al., 2003). A compilation of 68 watersheds on granitoid rocks at highly contrasted runoff  
483 and temperatures demonstrated a Si weathering flux that ranged within less than an order of  
484 magnitude (White and Blum, 1995). The magnitude of these natural variations are much  
485 lower than the ranges of Si release rates in laboratory experiments on various rocks and  
486 individual minerals. Indeed, the laboratory-based dissolution rates of silicate minerals ( $R_{Si}$ )  
487 range over more than 4 orders of magnitude at circum-neutral pH, depending on the identity  
488 of mineral (see Schott et al., 2009 and Heřmanská et al., 2022 for reviews). We therefore  
489 hypothesize, that, in addition in incontestable control on Si export fluxes of transport  
490 processes such as fluid residence time and flow rates (Maher, 2010) and biological processes  
491 such as plant uptake and litter decay (Lucas et al., 1993; Derry et al., 2005; Gérard et al.,  
492 2008; Fraysse et al., 2010), the topsoil itself may exert a major “buffering” effect on Si export  
493 from the watershed. By virtue of its silicate minerals, notably short-range order clays, labile  
494 Si pool and low sensibility of  $R_{Si}$  to the identity of soil and fluid pH, the soils across the world  
495 may regulate Si release rate at some ‘universal’ rate which is further reflected in relatively  
496 narrow range of riverine Si concentration and export flux. The latter is primarily dependent on  
497 river runoff rather than soil type and land use of the watershed.

498 In this regard, reactive transport and biogeochemical modeling of Si (and related  
499 elements) cycle in the system ‘rock-soil-river watershed’ (i.e., Godderis et al., 2019) should  
500 incorporate the reactivity of soils based on experimental data of the whole soil rather than  
501 individual constituting minerals. Consideration of superposition of known dissolution rates of  
502 primary and secondary soil minerals, routinely used in such modeling, instead of  
503 experimentally-measured whole soil rates may underestimate Si release (and thus, relevant  
504 concentrations in surface fluids) by 1 to 2 orders of magnitude. As such, experimental  
505 measurements of labile Si in various soils across the world, using flow-through reactors with  
506 both soil powder and soil column are needed.

## 507 **5. CONCLUDING REMARKS**

508 Dynamic mixed-flow and column laboratory experiments of soil dissolution in  
509 aqueous solutions revealed similar behaviour for different type of soils developed on  
510 calcareous or loess parent materials (calcaric cambisol, hypereutric cambisol, albeluvisol and  
511 luvisol) suggesting similar mechanisms responsible for release of Si ( $R_{Si}$ ) from the bulk of soil  
512 mineral matrix. The  $R_{Si}$  of studied soils was 1 to 2 orders of magnitude higher than that of  
513 common soil clays, and 1 to 3 orders of magnitude lower than that of plant phytoliths.  
514 Moreover, in contrast to clays and biogenic silica, the  $R_{Si}$  of whole soils weakly depended on  
515 pH at  $4 < \text{pH} < 8$  (decreased by a factor 1.5 to 2 for hypereutric cambisol and calcaric  
516 cambisol; independent for luvisol, and increasing 2-fold for albeluvisol). As such, the two  
517 dominant ‘bulk’ pools of Si cannot explain the magnitude and pH-dependence of its release  
518 rate from soils. We hypothesize that either amorphous allophanes, imogolite, organo-Fe-Al-Si  
519 compounds (poorly known from the view point of dissolution kinetics), or Si desorption from  
520 common soil minerals (Fe and Al hydroxides) can be responsible for labile Si pool released  
521 from soil into aqueous solution. This pool of reactive Si amounted to  $0.04\text{-}0.08 \text{ mg Si g}_{\text{soil}}^{-1}$

522 which is largely sufficient to provide the Si requirements of common plants in forest soils,  
523 and it can be mobilized into aqueous solution within first hours of contact with the fluid.

524 The reactivity of soils measured in this study demonstrates that very small fraction of  
525 actual soil present at the watershed (< 0.1-1%) is capable to provide the observed Si  
526 concentration in soil porewater and Si export flux from the watershed. Although we studied  
527 only limited number of soils, developed on loesses and calcareous substrates, we observed  
528 rather similar values of Si release rate regardless of the soil type, agricultural use, and solution  
529 pH. This may help to explain relatively low range of Si concentrations and fluxes observed in  
530 natural watersheds, compared to drastic differences in reactivity of individual silicate minerals  
531 or whole mother rocks inferred from laboratory experiments. Therefore, results obtained in  
532 the present study contribute to quantifying bulk soil reactivity with respect to Si release rate.  
533 We suggest that  $R_{Si}$  of whole soil, rather than that of individual soil minerals and amorphous  
534 (biogenic) silica, is better suited for being incorporated in existing reactive transport/chemical  
535 weathering models. This calls a need for experimental measurements of labile Si in various  
536 soils across the world, ideally using flow-through reactors.

537

538

### 539 **Acknowledgements**

540 Support from ANR BioSiSol is acknowledged. We thank A. Castillo for B.E.T. specific  
541 surface area measurements. OP and AL acknowledge support from the TSU Development  
542 Programme 'Priority-2030'.

543

### **REFERENCES**

- 544 Babu, T., Tubana, B., Paye, W., Kanke, Y., Datnoff, L., 2016. Establishing Soil Silicon Test  
545 Procedure and Critical Silicon Level for Rice in Louisiana Soils. *Commun. Soil Sci.*  
546 *Plant Anal.* 47, 1578–1597. <https://doi.org/10.1080/00103624.2016.1194996>  
547 Barão, L., Teixeira, R., Vandevenne, F., Ronchi, B., Unzué-Belmonte, D., Struyf, E., 2020.  
548 Silicon Mobilization in Soils: the Broader Impact of Land Use. *Silicon* 12, 1529–1538.  
549 <https://doi.org/10.1007/s12633-019-00245-y>  
550 Beckwith, R.S., Reeve, R., 1964. Studies on soluble silica in soils. II. The release of  
551 monosilicic acid from soils. *Soil Res.* 2, 33–45. <https://doi.org/10.1071/sr9640033>

- 552 Beckwith, R.S., Reeve, R., 1963. Studies on soluble silica in soils. I. The sorption of silicic  
553 acid by soils and minerals. *Soil Res.* 1, 157. <https://doi.org/10.1071/SR9630157>
- 554 Blum, W.E.H., Schad, P., Nortcliff, S., 2018. *Essentials of Soil Science Soil formation,*  
555 *functions, use and classification (World Reference Base, WRB).* Schweizerbart  
556 Science Publishers, Stuttgart, Germany.
- 557 Brinkman, R., 1970. Ferrolysis, a hydromorphic soil forming process. *Geoderma* 3, 199–206.  
558 [https://doi.org/10.1016/0016-7061\(70\)90019-4](https://doi.org/10.1016/0016-7061(70)90019-4)
- 559 Bruun Hansen, H.C., Raben-Lange, B., Raulund-Rasmussen, K., Borggaard, O.K., 1994.  
560 Monosilicate adsorption by ferrihydrite and goethite at pH 3–6. *Soil Sci.* 40–46.  
561 <https://doi.org/10.1097/00010694-199407000-00005>
- 562 Caubet, M., Cornu, S., Saby, N.P.A., Meunier, J.-D., 2020. Agriculture increases the  
563 bioavailability of silicon, a beneficial element for crop, in temperate soils. *Sci. Rep.*  
564 10, 19999. <https://doi.org/10.1038/s41598-020-77059-1>
- 565 Chesworth, W., Camps Arbestain, M., Macías, F., Spaargaren, O., Spaargaren, O., Mualem,  
566 Y., Morel- Seytoux, H.J., Horwath, W.R., Almendros, G., Chesworth, W., Grossl,  
567 P.R., Sparks, D.L., Spaargaren, O., Fairbridge, R.W., Singer, A., Eswaran, H.,  
568 Micheli, E., 2008. Classification of Soils: World Reference Base (WRB) for soil  
569 resources, in: Chesworth, W. (Ed.), *Encyclopedia of Soil Science*, Encyclopedia of  
570 Earth Sciences Series. Springer Netherlands, Dordrecht. [https://doi.org/10.1007/978-1-4020-3995-9\\_104](https://doi.org/10.1007/978-1-4020-3995-9_104)
- 571
- 572 Cho, Y., Driscoll, C.T., Johnson, C.E., Siccama, T.G., 2010. Chemical changes in soil and  
573 soil solution after calcium silicate addition to a northern hardwood forest.  
574 *Biogeochemistry* 3–20. <https://doi.org/10.1007/s10533-009-9397-6>
- 575 Chupakov, A.V., Pokrovsky, O.S., Moreva, O.Y., Shirokova, L.S., Neverova, N.V.,  
576 Chupakova, A.A., Kotova, E.I., Vorobyeva, T.Y., 2020. High resolution multi-annual  
577 riverine fluxes of organic carbon, nutrient and trace element from the largest European  
578 Arctic river, Severnaya Dvina. *Chem. Geol.* 538, 119491.  
579 <https://doi.org/10.1016/j.chemgeo.2020.119491>
- 580 Cooke, J., Leishman, M.R., 2016. Consistent alleviation of abiotic stress with silicon addition:  
581 a meta-analysis. *Funct. Ecol.* 30, 1340–1357. <https://doi.org/10.1111/1365-2435.12713>
- 582 Cornelis, J.-T., Delvaux, B., 2016. Soil processes drive the biological silicon feedback loop.  
583 *Funct. Ecol.* 30, 1298–1310. <https://doi.org/10.1111/1365-2435.12704>
- 584 Cornelis, J.-T., Delvaux, B., Georg, R.B., Lucas, Y., Ranger, J., Opfergelt, S., 2011. Tracing  
585 the origin of dissolved silicon transferred from various soil-plant systems towards  
586 rivers: a review. *Biogeosciences* 8, 89–112. <https://doi.org/10.5194/bg-8-89-2011>
- 587 Cornu, S., Lucas, Y., Desjardins, T., Nitsche, S., 1995. Rapid weathering kinetics of  
588 secondary minerals in forest ferralsols of Central Amazonia: bag-mineral method.  
589 *Comptes Rendus Acad. Sci. Ser. 2a Sci. Terre Planetes Fr.* 311–316.
- 590 Cornu, S., Meunier, J.-D., Ratie, C., Ouedraogo, F., Lucas, Y., Merdy, P., Barboni, D.,  
591 Delvigne, C., Borschneck, D., Grauby, O., Keller, C., 2022. Allophanes, a significant  
592 soil pool of silicon for plants. *Geoderma* 412, 115722.  
593 <https://doi.org/10.1016/j.geoderma.2022.115722>
- 594 Coskun, D., Deshmukh, R., Sonah, H., Menzies, J.G., Reynolds, O., Ma, J.F., Kronzucker,  
595 H.J., Bélanger, R.R., 2019. The controversies of silicon's role in plant biology. *New*  
596 *Phytol.* 221, 67–85. <https://doi.org/10.1111/nph.15343>
- 597 de Tombeur, F., Turner, B.L., Laliberté, E., Lambers, H., Mahy, G., Faucon, M.-P., Zemunik,  
598 G., Cornelis, J.-T., 2020. Plants sustain the terrestrial silicon cycle during ecosystem  
599 retrogression. *Science* 369, 1245–1248. <https://doi.org/10.1126/science.abc0393>



600 Delstanche, S., Opfergelt, S., Cardinal, D., Elsass, F., André, L., Delvaux, B., 2009. Silicon  
601 isotopic fractionation during adsorption of aqueous monosilicic acid onto iron oxide.  
602 *Geochim. Cosmochim. Acta* 73, 923–934. <https://doi.org/10.1016/j.gca.2008.11.014>

603 Derry, L.A., Kurtz, A.C., Ziegler, K., Chadwick, O.A., 2005. Biological control of terrestrial  
604 silica cycling and export fluxes to watersheds. *Nature* 433, 728–731.  
605 <https://doi.org/10.1038/nature03299>

606 Desplanques, V., Cary, L., Mouret, J.-C., Trolard, F., Bourrié, G., Grauby, O., Meunier, J.-D.,  
607 2006. Silicon transfers in a rice field in Camargue (France). *J. Geochem. Explor.* 88,  
608 190–193. <https://doi.org/10.1016/j.gexplo.2005.08.036>

609 Dietzel, M., 2002. Interaction of polysilicic and monosilicic acid with mineral surfaces, in:  
610 Stober, I., Bucher, K. (Eds.), *Water-Rock Interaction, Water Science and Technology*  
611 *Library*. Springer Netherlands, Dordrecht, pp. 207–235. [https://doi.org/10.1007/978-](https://doi.org/10.1007/978-94-010-0438-1_9)  
612 [94-010-0438-1\\_9](https://doi.org/10.1007/978-94-010-0438-1_9)

613 Farmer, V.C., Russell, J.D., Berrow, M.L., 1980. Imogolite and Proto-Imogolite Allophane in  
614 Spodic Horizons: Evidence for a Mobile Aluminium Silicate Complex in Podzol  
615 Formation. *J. Soil Sci.* 31, 673–684. [https://doi.org/10.1111/j.1365-](https://doi.org/10.1111/j.1365-2389.1980.tb02113.x)  
616 [2389.1980.tb02113.x](https://doi.org/10.1111/j.1365-2389.1980.tb02113.x)

617 Fraysse, F., Pokrovsky, O.S., Meunier, J.D., 2010. Experimental study of terrestrial plant litter  
618 interaction with aqueous solutions. *Geochim. Cosmochim. Acta* 74, 70–84.  
619 <https://doi.org/10.1016/j.gca.2009.09.002>

620 Fraysse, F., Pokrovsky, O.S., Schott, J., Meunier, J.-D., 2009. Surface chemistry and  
621 reactivity of plant phytoliths in aqueous solutions. *Chem. Geol.* 258, 197–206.  
622 <https://doi.org/10.1016/j.chemgeo.2008.10.003>

623 Fraysse, F., Pokrovsky, O.S., Schott, J., Meunier, J.-D., 2006. Surface properties, solubility  
624 and dissolution kinetics of bamboo phytoliths. *Geochim. Cosmochim. Acta* 70, 1939–  
625 1951. <https://doi.org/10.1016/j.gca.2005.12.025>

626 Gaillardet, J., Dupré, B., Louvat, P., Allègre, C.J., 1999. Global silicate weathering and CO<sub>2</sub>  
627 consumption rates deduced from the chemistry of large rivers. *Chem. Geol.* 159, 3–30.  
628 [https://doi.org/10.1016/S0009-2541\(99\)00031-5](https://doi.org/10.1016/S0009-2541(99)00031-5)

629 Gérard, F., Mayer, K.U., Hodson, M.J., Ranger, J., 2008. Modelling the biogeochemical cycle  
630 of silicon in soils: Application to a temperate forest ecosystem. *Geochim. Cosmochim.*  
631 *Acta* 72, 741–758. <https://doi.org/10.1016/j.gca.2007.11.010>

632 Goddérés, Y., Schott, J., Brantley, S.L., 2019. Reactive Transport Models of Weathering.  
633 *Elements* 15, 103–106. <https://doi.org/10.2138/gselements.15.2.103>

634 Golubev, S.V., Bauer, A., Pokrovsky, O.S., 2006. Effect of pH and organic ligands on the  
635 kinetics of smectite dissolution at 25°C. *Geochim. Cosmochim. Acta* 70, 4436–4451.  
636 <https://doi.org/10.1016/j.gca.2006.06.1557>

637 Haynes, R.J., 2017. Chapter Three - Significance and Role of Si in Crop Production, in:  
638 Sparks, D.L. (Ed.), *Advances in Agronomy*. Academic Press, pp. 83–166.  
639 <https://doi.org/10.1016/bs.agron.2017.06.001>

640 Haynes, R.J., Zhou, Y.-F., 2020. Silicate sorption and desorption by a Si-deficient soil –  
641 Effects of pH and period of contact. *Geoderma* 365, 114204.  
642 <https://doi.org/10.1016/j.geoderma.2020.114204>

643 Haysom, M.B.C., Chapman, L.S., 1975. Some aspects of the calcium silicate trials at Mackay.  
644 *Proc Qld Soc Sugar Cane Technol* 117–122.

645 Hedin, L.O., Vitousek, P.M., Matson, P.A., 2003. Nutrient losses over four million years of  
646 tropical forest development. *Ecology* 84, 2231–2255. <https://doi.org/10.1890/02-4066>

647 Heřmanská, M., Voigt, M.J., Marieni, C., Declercq, J., Oelkers, E.H., 2022. A comprehensive  
648 and internally consistent mineral dissolution rate database: Part I: Primary silicate

649 minerals and glasses. *Chem. Geol.* 597, 120807.  
650 <https://doi.org/10.1016/j.chemgeo.2022.120807>

651 Hingston, F.J., Raupach, M., 1967. The reaction between monosilicic acid and aluminium  
652 hydroxide. I. Kinetics of adsorption of silicic acid by aluminium hydroxide. *Soil Res.*  
653 5, 295–309. <https://doi.org/10.1071/sr9670295>

654 Keller, C., Rizwan, M., Meunier, J.-D., 2021. Are clay minerals a significant source of Si for  
655 crops? A Comparison of amorphous silica and the roles of the mineral type and pH.  
656 *Silicon* 13, 3611–3618. <https://doi.org/10.1007/s12633-020-00877-5>

657 Klotzbücher, T., Marxen, A., Vetterlein, D., Schneiker, J., Türke, M., van Sinh, N., Manh,  
658 N.H., van Chien, H., Marquez, L., Villareal, S., Bustamante, J.V., Jahn, R., 2015.  
659 Plant-available silicon in paddy soils as a key factor for sustainable rice production in  
660 Southeast Asia. *Basic Appl. Ecol.* 16, 665–673.  
661 <https://doi.org/10.1016/j.baae.2014.08.002>

662 Köhler, S.J., Bosbach, D., Oelkers, E.H., 2005. Do clay mineral dissolution rates reach steady  
663 state? *Geochim. Cosmochim. Acta* 69, 1997–2006.  
664 <https://doi.org/10.1016/j.gca.2004.10.015>

665 Köhler, S.J., Dufaud, F., Oelkers, E.H., 2003. An experimental study of illite dissolution  
666 kinetics as a function of pH from 1.4 to 12.4 and temperature from 5 to 50°C.  
667 *Geochim. Cosmochim. Acta* 67, 3583–3594. [https://doi.org/10.1016/S0016-7037\(03\)00163-7](https://doi.org/10.1016/S0016-7037(03)00163-7)

669 Kolesnikov, M.P., Gins, V.K., 2001. Forms of silicon in medicinal plants. *Appl. Biochem.*  
670 *Microbiol.* 37, 524–527. <https://doi.org/10.1023/A:1010262527643>

671 Landré, A., Cornu, S., Meunier, J.-D., Guerin, A., Arrouays, D., Caubet, M., Ratié, C., Saby,  
672 N.P.A., 2020. Do climate and land use affect the pool of total silicon concentration? A  
673 digital soil mapping approach of French topsoils. *Geoderma* 364, 114175.  
674 <https://doi.org/10.1016/j.geoderma.2020.114175>

675 Li, Z., Meunier, J.-D., Delvaux, B., 2022. Aggregation reduces the release of bioavailable  
676 silicon from allophane and phytolith. *Geochim. Cosmochim. Acta* 325, 87–105.  
677 <https://doi.org/10.1016/j.gca.2022.03.025>

678 Lowson, R.T., Comarmond, M.-C.J., Rajaratnam, G., Brown, P.L., 2005. The kinetics of the  
679 dissolution of chlorite as a function of pH and at 25°C. *Geochim. Cosmochim. Acta*  
680 69, 1687–1699. <https://doi.org/10.1016/j.gca.2004.09.028>

681 Lucas, Y., 2001. The role of plants in controlling rates and products of weathering:  
682 Importance of biological pumping. *Annu. Rev. Earth Planet. Sci.* 29, 135–163.  
683 <https://doi.org/10.1146/annurev.earth.29.1.135>

684 Lucas, Y., Luizao, F.J., Chauvel, A., Rouiller, J., Nahon, D., 1993. The relation between  
685 biological activity of the rain forest and mineral composition of soils. *Science* 260,  
686 521–523. <https://doi.org/10.1126/science.260.5107.521>

687 Maher, K., 2010. The dependence of chemical weathering rates on fluid residence time. *Earth*  
688 *Planet. Sci. Lett.* 294, 101–110. <https://doi.org/10.1016/j.epsl.2010.03.010>

689 Matichenkov, V.V., Snyder, G.H., 1996. The mobile silicon compounds in some South  
690 Florida soils. *Eurasian Soil Sci.* 1165–1180.

691 McKeague, J.A., Cline, M.G., 1963. Silica in soil solutions: ii: the adsorption of monosilicic  
692 acid by soil and by other substances. *Can. J. Soil Sci.* 43, 83–96.  
693 <https://doi.org/10.4141/cjss63-011>

694 Merdy, P., Meunier, J.-D., Ziarelli, F., Lucas, Y., 2022. Evidence of humic acid-  
695 aluminium- silicon complexes under controlled conditions. *Sci. Total Environ.* 829,  
696 154601. <https://doi.org/10.1016/j.scitotenv.2022.154601>

697 Meunier, J.D., Barboni, D., Anwar-ul-Haq, M., Levard, C., Chaurand, P., Vidal, V., Grauby,  
698 O., Huc, R., Laffont-Schwob, I., Rabier, J., Keller, C., 2017. Effect of phytoliths for

699 mitigating water stress in durum wheat. *New Phytol.* 215, 229–239.  
700 <https://doi.org/10.1111/nph.14554>

701 Meunier, J.-D., Colin, F., Alarcon, C., 1999. Biogenic silica storage in soils. *Geology* 27,  
702 835–838. <https://doi.org/10.1130/0091-7613>.

703 Meunier, J.-D., Cornu, S., Keller, C., Barboni, D., 2022. The role of silicon in the supply of  
704 terrestrial ecosystem services. *Environ. Chem. Lett.* 20, 2109–2121.  
705 <https://doi.org/10.1007/s10311-021-01376-8>

706 Meunier, J.-D., Sandhya, K., Prakash, N.B., Borschneck, D., Dussouillez, P., 2018. pH as a  
707 proxy for estimating plant-available Si? A case study in rice fields in Karnataka (South  
708 India). *Plant Soil* 432, 143–155. <https://doi.org/10.1007/s11104-018-3758-7>

709 Narayanaswamy, C., Prakash, N.B., 2010. Evaluation of selected extractants for plant-  
710 available silicon in rice soils of Southern India. *Commun. Soil Sci. Plant Anal.* 41,  
711 977–989. <https://doi.org/10.1080/00103621003646063>

712 Oliva, P., Viers, J., Dupré, B., 2003. Chemical weathering in granitic environments. *Chem.*  
713 *Geol.* 202, 225–256. <https://doi.org/10.1016/j.chemgeo.2002.08.001>

714 Phillips, A.K., Cowling, S.A., 2019. Biotic and abiotic controls on watershed Si cycling and  
715 river Si yield in western Canada. *Biogeochemistry* 143, 221–237.  
716 <https://doi.org/10.1007/s10533-019-00557-6>

717 Pokrovsky, O.S., Dupré, B., Schott, J., 2005a. Fe–Al–organic Colloids Control of Trace  
718 Elements in Peat Soil Solutions: Results of Ultrafiltration and Dialysis. *Aquat.*  
719 *Geochem.* 11, 241–278. <https://doi.org/10.1007/S10498-004-4765-2>

720 Pokrovsky, O.S., Manasypov, R.M., Kopysov, S.G., Krickov, I.V., Shirokova, L.S., Loiko,  
721 S.V., Lim, A.G., Kolesnichenko, L.G., Vorobyev, S.N., Kirpotin, S.N., 2020. Impact  
722 of permafrost thaw and climate warming on riverine export fluxes of carbon, nutrients  
723 and metals in Western Siberia. *Water Switz.* 12, 1817.  
724 <https://doi.org/10.3390/w12061817>

725 Pokrovsky, O.S., Schott, J., Kudryavtzev, D.I., Dupré, B., 2005b. Basalt weathering in  
726 Central Siberia under permafrost conditions. *Geochim. Cosmochim. Acta* 69, 5659–  
727 5680. <https://doi.org/10.1016/j.gca.2005.07.018>

728 Pokrovsky, O.S., Shirokova, L.S., Benezeth, P., Schott, J., Golubev, S.V., 2009. Effect of  
729 organic ligands and heterotrophic bacteria on wollastonite dissolution kinetics. *Am. J.*  
730 *Sci.* 309, 731–772. <https://doi.org/10.2475/08.2009.05>

731 Pokrovsky, O.S., Shirokova, L.S., Zabelina, S.A., Jordan, G., Benezeth, P., 2021. Weak  
732 impact of microorganisms on Ca, Mg-bearing silicate weathering. *NPJ Materials*  
733 *Degradation*, 5, Art No 51. <https://doi.org/10.1038/s41529-021-00199-w>.

734 Puppe, D., Ehrmann, O., Kaczorek, D., Wanner, M., Sommer, M., 2015. The protozoic Si  
735 pool in temperate forest ecosystems — Quantification, abiotic controls and  
736 interactions with earthworms. *Geoderma* 243–244, 196–204.  
737 <https://doi.org/10.1016/j.geoderma.2014.12.018>

738 Ralston, S.J., Hausrath, E.M., Tschauer, O., Rampe, E., Peretyazhko, T.S., Christoffsen, R.,  
739 Defelice, C., Lee, H., 2021. Dissolution rates of allophane with variable Fe contents:  
740 implications for aqueous alteration and the preservation of X-RAY amorphous  
741 materials on Mars. *Clays Clay Miner.* 69, 263–288. <https://doi.org/10.1007/s42860-021-00124-x>

743 Richard Drees, L., Wilding, L.P., Smeck, N.E., Senkayi, A.L., 1989. Silica in Soils: Quartz  
744 and Disordered Silica Polymorphs, in: *Minerals in Soil Environments*. John Wiley &  
745 Sons, Ltd, pp. 913–974. <https://doi.org/10.2136/sssabookser1.2ed.c19>

746 Ronchi, B., Barão, L., Clymans, W., Vandevenne, F., Batelaan, O., Govers, G., Struyf, E.,  
747 Dassargues, A., 2015. Factors controlling Si export from soils: A soil column  
748 approach. *Catena* 133, 85–96. <https://doi.org/10.1016/j.catena.2015.05.007>

- 749 Ronchi, B., Clymans, W., Barão, A.L.P., Vandevenne, F., Struyf, E., Batelaan, O.,  
750 Dassargues, A., Govers, G., 2013. Transport of Dissolved Si from Soil to River: A  
751 Conceptual Mechanistic Model. *Silicon* 5, 115–133. [https://doi.org/10.1007/s12633-](https://doi.org/10.1007/s12633-012-9138-7)  
752 [012-9138-7](https://doi.org/10.1007/s12633-012-9138-7)
- 753 Rozalén, M.L., Huertas, F.J., Brady, P.V., Cama, J., García-Palma, S., Linares, J., 2008.  
754 Experimental study of the effect of pH on the kinetics of montmorillonite dissolution  
755 at 25°C. *Geochim. Cosmochim. Acta* 72, 4224–4253.  
756 <https://doi.org/10.1016/j.gca.2008.05.065>
- 757 Rückert, E., 1992. Naßbleichung und Tonzerstörung durch Ferrolisis in Stauwasserböden  
758 Baden-Württembergs? *Hohenheimer Bodenkundliche Hefte* 3, 1–178.
- 759 Schaller, J., Puppe, D., Kaczorek, D., Ellerbrock, R., Sommer, M., 2021. Silicon Cycling in  
760 Soils Revisited. *Plants* 10, 295. <https://doi.org/10.3390/plants10020295>
- 761 Schott, J., Pokrovsky, O.S., Oelkers, E.H., 2009. The Link Between Mineral  
762 Dissolution/Precipitation Kinetics and Solution Chemistry. *Rev. Mineral. Geochem.*  
763 70, 207–258. <https://doi.org/10.2138/rmg.2009.70.6>
- 764 Sigg, L., Stumm, W., 1981. The interaction of anions and weak acids with the hydrous  
765 goethite ( $\alpha$ -FeOOH) surface. *Colloids Surf.* 2, 101–117. [https://doi.org/10.1016/0166-](https://doi.org/10.1016/0166-6622(81)80001-7)  
766 [6622\(81\)80001-7](https://doi.org/10.1016/0166-6622(81)80001-7)
- 767 Sommer, M., Kaczorek, D., Kuzyakov, Y., Breuer, J., 2006. Silicon pools and fluxes in soils  
768 and landscapes—a review. *J. Plant Nutr. Soil Sci.* 169, 310–329.  
769 <https://doi.org/10.1002/jpln.200521981>
- 770 Tubana, B.S., Babu, T., Datnoff, L.E., 2016. A Review of Silicon in Soils and Plants and Its  
771 Role in US Agriculture: History and Future Perspectives. *Soil Sci.* 181, 393.  
772 <https://doi.org/10.1097/SS.0000000000000179>
- 773 Ugolini, F.C., Dahlgren, R.A., 2002. Soil Development in Volcanic Ash. *Glob. Environ. Res.*  
774 69–82.
- 775 Vandekerckhove, E., Bertrand, S., Reid, B., Bartels, A., Charlier, B., 2016. Sources of  
776 dissolved silica to the fjords of northern Patagonia (44–48°S): the importance of  
777 volcanic ash soil distribution and weathering. *Earth Surf. Process. Landf.* 41, 499–512.  
778 <https://doi.org/10.1002/esp.3840>
- 779 Vempati, R.K., Loeppert, R.H., 1989. Influence of Structural and Adsorbed Si on the  
780 Transformation of Synthetic Ferrihydrite. *Clays Clay Miner.* 37, 273–279.  
781 <https://doi.org/10.1346/CCMN.1989.0370312>
- 782 Watteau, F., Villemin, G., 2001. Ultrastructural study of the biogeochemical cycle of silicon  
783 in the soil and litter of a temperate forest. *Eur. J. Soil Sci.* 52, 385–396.  
784 <https://doi.org/10.1046/j.1365-2389.2001.00391.x>
- 785 Watteau, F., Villemin, G., Ghanbaja, J., Genet, P., Pargney, J.-C., 2002. In situ ageing of fine  
786 beech roots (*Fagus sylvatica*) assessed by transmission electron microscopy and  
787 electron energy loss spectroscopy: description of microsites and evolution of  
788 polyphenolic substances. *Biol. Cell* 94, 55–63. [https://doi.org/10.1016/S0248-](https://doi.org/10.1016/S0248-4900(02)01182-6)  
789 [4900\(02\)01182-6](https://doi.org/10.1016/S0248-4900(02)01182-6)
- 790 White, A.F., Blum, A.E., 1995. Effects of climate on chemical\_ weathering in watersheds.  
791 *Geochim. Cosmochim. Acta* 59, 1729–1747. [https://doi.org/10.1016/0016-](https://doi.org/10.1016/0016-7037(95)00078-E)  
792 [7037\(95\)00078-E](https://doi.org/10.1016/0016-7037(95)00078-E)
- 793 Yang, S., Hao, Q., Liu, H., Zhang, X., Yu, C., Yang, X., Xia, S., Yang, W., Li, J., Song, Z.,  
794 2019. Impact of grassland degradation on the distribution and bioavailability of soil  
795 silicon: Implications for the Si cycle in grasslands. *Sci. Total Environ.* 657, 811–818.  
796 <https://doi.org/10.1016/j.scitotenv.2018.12.101>
- 797 Yang, X., Song, Z., Yu, C., Ding, F., 2020. Quantification of different silicon fractions in  
798 broadleaf and conifer forests of northern China and consequent implications for

799 biogeochemical Si cycling. Geoderma 361, 114036.  
 800 <https://doi.org/10.1016/j.geoderma.2019.114036>  
 801 Zakharova, E.A., Pokrovsky, O.S., Dupré, B., Gaillardet, J., Efimova, L.E., 2007. Chemical  
 802 weathering of silicate rocks in Karelia region and Kola peninsula, NW Russia:  
 803 Assessing the effect of rock composition, wetlands and vegetation. Chem. Geol. 242,  
 804 255–277. <https://doi.org/10.1016/j.chemgeo.2007.03.018>  
 805 Zakharova, E.A., Pokrovsky, O.S., Dupré, B., Zaslavskaya, M.B., 2005. Chemical weathering  
 806 of silicate rocks in Aldan Shield and Baikal Uplift: insights from long-term seasonal  
 807 measurements of solute fluxes in rivers. Chem. Geol. 214, 223–248.  
 808 <https://doi.org/10.1016/j.chemgeo.2004.10.003>  
 809  
 810  
 811  
 812  
 813  
 814  
 815  
 816  
 817  
 818  
 819  
 820  
 821

822 **Table 1.** Soil origin, description, physical and chemical properties. More information is  
 823 provided in Cornu et al. (2022). The soils are ordered as following: first the soil developed in  
 824 calcareous rock containing carbonates, then those in which carbonates were dissolved, then  
 825 soils developed in loess, with the most evolved at the end (albeluvisol). SOC is Soil Organic  
 826 Carbon and SSA is Specific Surface Area.  
 827

Soil type (WRB, 2006)	Sample I.D.	Sampling depth, cm <sup>(*)</sup>	SOC, g kg <sup>-1</sup> (*)	pH (*)	< 2 μm g kg <sup>-1</sup> (*)	SSA, m <sup>2</sup> /g
Calcaric	701C1	0-20	47	7.9	491	
Cambisol	701F1	0-20	53	6.8	477	
Calcaric	755C1	0-20	23	8.1	514	49.1
Cambisol	755F1	0-10	69	6.9	695	22.8
	755F2	10-20	39	7.7	514	
Hypereutric Cambisol	BS2C1	0-25	14	8.1	307	17.8
	BS2F1	0-10	39	5.9	282	14.2
	BS2F2	10-25	24	6.1	307	
Hypereutric Cambisol	1166C1	0-25	17	7.3	341	19.2
	1166F1	0-5	45	6.9	376	19.2
	1166F2	5-20	25	6.9	371	

Luvisol	340C1	0-25	11	7.0	156	12.6
	340F1	0-10	23	5.1	136	22.8
	340F2	10-25	11	5.0	134	
Luvisol	62C1	0-25	11	8.0	195	8.05
	62F1	0-5	29	4.1	162	6.11
	62F2	5-35	9.6	4.4	152	
Albeluvisol	BS3C1	0-20	9.5	7.1	160	10.5
	BS3F1	0-15	24	5.3	110	13.5
	BS3F2	15-25	12	4.9	108	

828

829 (\*) Cornu et al. (2022)

830

831

832 **Table 2.** Si-based dissolution rates of soils determined in mixed-flow reactors. Here and  
833 below, bicarbonate is 10 mM NaCl +1 mM NaHCO<sub>3</sub>; acetate is 5 mM NaCl+5 mM acetic  
834 acid. The pH values are measured in the outlet solutions, which corresponds to the steady-  
835 state conditions of the dissolution process.

836

Soil type	Fluid	Duration, h	pH	R <sub>Si</sub> , mol/g <sub>soil</sub> /h	S.D. R <sub>Si</sub>	R <sub>Si</sub> , mol/m <sup>2</sup> /d	S.D. R <sub>Si</sub>
Calcaric cambisol 701C1	MQ	260	7.13	4.6×10 <sup>-8</sup>	1.2×10 <sup>-8</sup>	-	-
	Bicarbonate	120	7.74	4.5×10 <sup>-8</sup>	3.4×10 <sup>-9</sup>	-	-
	Acetate	132	4.29	1.1×10 <sup>-7</sup>	4.2×10 <sup>-9</sup>	-	-
Calcaric cambisol 701F1	MQ	260	6.72	2.7×10 <sup>-8</sup>	6.6×10 <sup>-9</sup>	-	-
	Bicarbonate	120	7.76	3.8×10 <sup>-8</sup>	3.9×10 <sup>-9</sup>	-	-
	Acetate	132	4.2	5.2×10 <sup>-8</sup>	1.8×10 <sup>-9</sup>	-	-
Calcaric cambisol 755C1	MQ	288	6.41	8.6×10 <sup>-8</sup>	6.5×10 <sup>-9</sup>	1.2×10 <sup>-8</sup>	2.9×10 <sup>-9</sup>
	Bicarbonate	204	7.84	7.3×10 <sup>-8</sup>	1.4×10 <sup>-9</sup>	3.6×10 <sup>-8</sup>	6.8×10 <sup>-9</sup>
	Acetate	312	4.25	1.2×10 <sup>-7</sup>	1.5×10 <sup>-8</sup>	6.1×10 <sup>-8</sup>	7.4×10 <sup>-9</sup>
	MQ	144	6.78	6.3×10 <sup>-8</sup>	3.5×10 <sup>-9</sup>	3.1×10 <sup>-8</sup>	1.7×10 <sup>-9</sup>
Calcaric cambisol 755F1	MQ	288	6.86	5.3×10 <sup>-8</sup>	3.6×10 <sup>-9</sup>	5.6×10 <sup>-8</sup>	3.8×10 <sup>-9</sup>
	Bicarbonate	204	7.78	5.9×10 <sup>-8</sup>	5.9×10 <sup>-9</sup>	6.2×10 <sup>-8</sup>	6.2×10 <sup>-9</sup>
	Acetate	312	4.27	1.2×10 <sup>-7</sup>	4.4×10 <sup>-9</sup>	1.3×10 <sup>-7</sup>	4.6×10 <sup>-9</sup>
	MQ	504	5.88	8.1×10 <sup>-8</sup>	1.2×10 <sup>-8</sup>	8.5×10 <sup>-8</sup>	1.3×10 <sup>-8</sup>
Hypereutric cambisol BS2C1	MQ	228	6.43	6.5×10 <sup>-8</sup>	3.1×10 <sup>-9</sup>	1.1×10 <sup>-7</sup>	5.3×10 <sup>-9</sup>
	Bicarbonate	216	7.78	6.4×10 <sup>-8</sup>	5.6×10 <sup>-9</sup>	1.1×10 <sup>-7</sup>	9.5×10 <sup>-9</sup>
Hypereutric cambisol BS2F1	MQ	228	6.62	7.4×10 <sup>-8</sup>	7.2×10 <sup>-9</sup>	1.2×10 <sup>-7</sup>	1.2×10 <sup>-8</sup>
	Bicarbonate	288	7.93	7.2×10 <sup>-8</sup>	8.6×10 <sup>-9</sup>	1.2×10 <sup>-7</sup>	1.4×10 <sup>-8</sup>
	Acetate	120	4.43	1.1×10 <sup>-7</sup>	1.2×10 <sup>-8</sup>	1.8×10 <sup>-7</sup>	2.1×10 <sup>-8</sup>
	MQ	96	6.41	5.1×10 <sup>-8</sup>	5.2×10 <sup>-9</sup>	8.6×10 <sup>-8</sup>	8.7×10 <sup>-9</sup>
Hypereutric cambisol 1166C1	MQ	288	6.59	6.3×10 <sup>-8</sup>	9.6×10 <sup>-9</sup>	7.9×10 <sup>-8</sup>	1.2×10 <sup>-8</sup>
	Bicarbonate	204	7.83	6.5×10 <sup>-8</sup>	1.2×10 <sup>-8</sup>	8.2×10 <sup>-8</sup>	1.5×10 <sup>-8</sup>
	Acetate	312	4.25	9.1×10 <sup>-8</sup>	5.8×10 <sup>-9</sup>	1.1×10 <sup>-7</sup>	7.3×10 <sup>-9</sup>
Hypereutric cambisol 1166F1	MQ	288	6.56	4.9×10 <sup>-8</sup>	4.7×10 <sup>-9</sup>	6.1×10 <sup>-8</sup>	5.8×10 <sup>-9</sup>
	Bicarbonate	204	7.91	6.7×10 <sup>-8</sup>	4.4×10 <sup>-9</sup>	8.4×10 <sup>-8</sup>	5.5×10 <sup>-9</sup>
	Acetate	312	4.26	8.7×10 <sup>-8</sup>	2.4×10 <sup>-9</sup>	1.1×10 <sup>-7</sup>	2.9×10 <sup>-9</sup>
	MQ	504	5.74	6.1×10 <sup>-8</sup>	6.7×10 <sup>-9</sup>	7.6×10 <sup>-8</sup>	8.4×10 <sup>-9</sup>
Luvisol 340F1	MQ	288	6.17	3.5×10 <sup>-8</sup>	1.2×10 <sup>-9</sup>	3.7×10 <sup>-8</sup>	1.3×10 <sup>-9</sup>
	Bicarbonate	204	7.85	4.7×10 <sup>-8</sup>	2.6×10 <sup>-9</sup>	4.9×10 <sup>-8</sup>	2.8×10 <sup>-9</sup>
	Acetate	24	4.29	5.7×10 <sup>-8</sup>	3.8×10 <sup>-9</sup>	6.1×10 <sup>-8</sup>	3.9×10 <sup>-9</sup>
Luvisol 340C1	MQ	312	5.57	4.4×10 <sup>-8</sup>	3.1×10 <sup>-9</sup>	4.6×10 <sup>-8</sup>	3.2×10 <sup>-9</sup>
	MQ	24	6.27	4.4×10 <sup>-8</sup>	5.2×10 <sup>-9</sup>	8.3×10 <sup>-8</sup>	9.9×10 <sup>-9</sup>
	Bicarbonate	12	7.93	6.4×10 <sup>-8</sup>	4.1×10 <sup>-9</sup>	1.2×10 <sup>-7</sup>	7.8×10 <sup>-9</sup>
	Acetate	24	4.26	1.1×10 <sup>-7</sup>	4.2×10 <sup>-9</sup>	2.1×10 <sup>-7</sup>	8.1×10 <sup>-9</sup>
Luvisol 62C1	MQ	312	5.74	4.2×10 <sup>-8</sup>	9.5×10 <sup>-9</sup>	7.9×10 <sup>-8</sup>	1.8×10 <sup>-9</sup>
	MQ	228	6.52	6.3×10 <sup>-8</sup>	5.8×10 <sup>-9</sup>	1.9×10 <sup>-7</sup>	1.7×10 <sup>-8</sup>
Luvisol	Bicarbonate	288	7.84	6.5×10 <sup>-8</sup>	4.5×10 <sup>-9</sup>	1.9×10 <sup>-7</sup>	1.3×10 <sup>-8</sup>
Luvisol	MQ	228	5.97	5.3×10 <sup>-8</sup>	1.9×10 <sup>-8</sup>	2.1×10 <sup>-7</sup>	7.6×10 <sup>-8</sup>

62F1	Bicarbonate	288	7.89	$6.8 \times 10^{-8}$	$4.6 \times 10^{-8}$	$2.7 \times 10^{-7}$	$6.3 \times 10^{-8}$
	Acetate	120	4.38	$6.2 \times 10^{-8}$	$2.4 \times 10^{-9}$	$2.4 \times 10^{-7}$	$9.2 \times 10^{-9}$
	MQ	96	6.16	$2.8 \times 10^{-8}$	$7.3 \times 10^{-9}$	$1.1 \times 10^{-7}$	$2.9 \times 10^{-8}$
Albeluvisol BS3C1 N50g	MQ	260	6.03	$2.1 \times 10^{-8}$	$4.8 \times 10^{-9}$	$2.9 \times 10^{-9}$	$6.9 \times 10^{-10}$
	Bicarbonate	120	7.9	$4.5 \times 10^{-8}$	$5.6 \times 10^{-9}$	$6.4 \times 10^{-9}$	$7.9 \times 10^{-10}$
	Acetate	132	4.1	$2.5 \times 10^{-8}$	$1.6 \times 10^{-9}$	$3.6 \times 10^{-9}$	$2.3 \times 10^{-10}$
Albeluvisol BS3F2 N37g	MQ	260	5.68	$2.3 \times 10^{-8}$	$3.8 \times 10^{-9}$	$2.9 \times 10^{-9}$	$4.7 \times 10^{-10}$
	Bicarbonate	120	8.16	$3.8 \times 10^{-8}$	$9.5 \times 10^{-9}$	$4.8 \times 10^{-9}$	$1.2 \times 10^{-9}$
	Acetate	132	4.11	$1.9 \times 10^{-8}$	$1.5 \times 10^{-8}$	$2.5 \times 10^{-9}$	$1.9 \times 10^{-9}$
Albeluvisol BS3F1 N47g	MQ	260	5.51	$1.7 \times 10^{-8}$	$3.4 \times 10^{-9}$	$1.9 \times 10^{-9}$	$3.8 \times 10^{-10}$
	Bicarbonate	120	8.14	$3.5 \times 10^{-8}$	$6.2 \times 10^{-9}$	$3.9 \times 10^{-9}$	$6.9 \times 10^{-10}$
	Acetate	132	4.06	$2.8 \times 10^{-8}$	$1.4 \times 10^{-9}$	$3.1 \times 10^{-10}$	$1.6 \times 10^{-10}$

837 Footnote : MQ is for Milli-Q, distilled water.

838  
839  
840  
841  
842  
843  
844  
845  
846  
847  
848  
849  
850  
851  
852  
853  
854  
855  
856  
857  
858  
859  
860  
861  
862  
863  
864  
865  
866  
867  
868  
869  
870  
871  
872  
873



874  
875  
876  
877  
878  
879  
880  
881

**Table 3.** Si release rates (mean  $\pm$  s.d.) determined in column-through experiments.

Soil type	Fluid	Duration, h	pH outlet	$R_{Si}$ , $\text{mol g}_{\text{soil}}^{-1} \text{d}^{-1}$
Calcaric cambisol	Milli-Q	240	6.26	$(3.7 \pm 2.3) \times 10^{-8}$
755 F1 (0.5 g) + 755 F2 (1.5 g)	Acetate	100	4.20*	$(6.5 \pm 0.79) \times 10^{-8}$
Hypereutric cambisol	Milli-Q	170	5.85	$(1.2 \pm 0.57) \times 10^{-8}$
1166 F1 (1 g) + 1166 F2 (3g)	Acetate	190	4.42	$(5.3 \pm 1.4) \times 10^{-8}$
Hypereutric cambisol	Milli-Q	170	5.07	$(1.7 \pm 1.4) \times 10^{-8}$
BS2 F1(1 g) + BS2 F2 (3g)	Milli-Q	170	5.26	$(6.9 \pm 6.8) \times 10^{-9}$
Luvisol	Milli-Q	170	5.26	$(6.9 \pm 6.8) \times 10^{-9}$
340 F1 (1 g) +	Acetate	190	4.05	$(1.1 \pm 0.19) \times 10^{-8}$
340 F2 (3 g)	Bicarbonate	390	7.95*	$(1.8 \pm 0.35) \times 10^{-9}$
Luvisol	Milli-Q	170	4.58	$(7.7 \pm 5.5) \times 10^{-9}$
62 F1 (1 g) +	Acetate	190	3.97	$(1.1 \pm 0.18) \times 10^{-8}$
62 F2 (3 g)	Bicarbonate	390	8.10*	$(2.6 \pm 2.2) \times 10^{-9}$

882  
883  
884  
885

\* Approximated based on results of mixed-flow reactors.

886  
887  
888  
889  
890  
891  
892  
893  
894  
895

896  
897  
898  
899  
900  
901

**Table 4.** Pools (mean  $\pm$  s.d.) of labile, fast-leaching Si determined by integration of Si breakthrough curves in soil column experiments over the first 100 h of reaction.

Soil type	Fluid	Time, h	pH outlet	Pool Si, mg kg <sub>soil</sub> <sup>-1</sup>
Calcaric cambisol 755 F1 (0.5 g) + 755 F2 (1.5 g)	MQ	0-10	6.47	45 $\pm$ 8.7
		10-100	6.11	100 $\pm$ 15
	Acetate	0-10	4.1*	103 $\pm$ 70
		10-100	4.2*	83 $\pm$ 4.9
Hypereutric cambisol 1166 F1(1 g) + 1166 F2 (3g)	MQ	0-10	6.75	48 $\pm$ 5.5
		10-100	5.46	36 $\pm$ 5.8
	Acetate	0-10	5.02	63 $\pm$ 32
		10-100	4.06	106 $\pm$ 10
Hypereutric cambisol BS2 F1 (1 g) + BS2 F2 (3 g)	MQ	0-10	5.25	40 $\pm$ 7.9
		10-100	4.98	31 $\pm$ 3.7
Luvisol 340 F1 (1 g) + F2 (3 g)	MQ	0-10	5.7	34 $\pm$ 13
		10-100	5.15	11 $\pm$ 2.1
	Acetate	0-10	4.16	3.0 $\pm$ 0.7
		10-100	3.98	21 $\pm$ 1.8
	Bicarbonate	0-10	7.85*	4.3 $\pm$ 2.4
		10-100	7.95*	5.1 $\pm$ 0.9
Luvisol 62 F1 (1 g) + F2 (3 g)	MQ	0-10	4.5	39 $\pm$ 15
		10-100	4.62	19 $\pm$ 2.5
	Acetate	0-10	3.98	2.4 $\pm$ 0.6
		10-100	3.98	15 $\pm$ 1.8
	Bicarbonate	0-10	7.9*	6.2 $\pm$ 4.2
		10-100	8.1*	21 $\pm$ 0.9

902  
903  
904  
905  
906  
907  
908  
909  
910

\* Approximated based on results of mixed-flow reactors.

911  
912  
913  
914  
915  
916  
917  
918

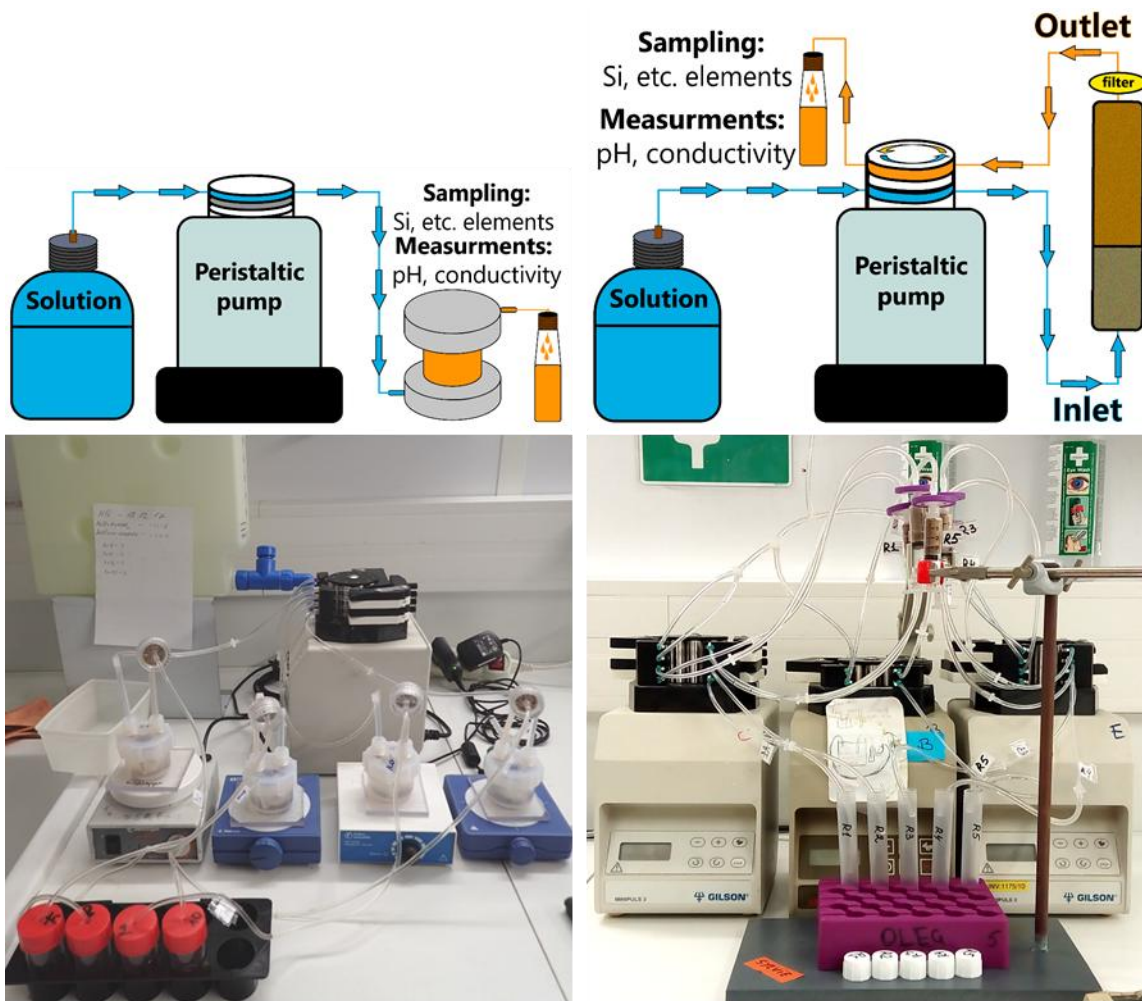
**Table 5.** Linear (Pearson) correlation matrix of pools of labile, fast-leaching Si and different Si forms in soils taken from Cornu et al. (2022). Significant correlations at  $p < 0.01$ , labelled by asterisk.

<b>Time period, h</b>	<b>Si<sub>tot</sub><sup>(1)</sup></b>	<b>Si<sub>O</sub><sup>(2)</sup></b>	<b>Si<sub>d</sub><sup>(3)</sup></b>	<b>Si<sub>CaCl2</sub><sup>(4)</sup></b>	<b>Phytoliths</b>
MQ 0-10 h	-0.72	0.73	0.68	0.94	-0.32
MQ 10-100 h	-0.98*	0.97*	0.93	0.73	-0.40
Acetate 0-10 h	-0.98*	0.99*	0.85	0.92*	-0.60
Acetate 10-100 h	-0.75	0.78	0.55	0.98*	-0.67

919  
920  
921  
922  
923  
924  
925  
926  
927  
928  
929  
930

Footnote:

- (1) Si<sub>tot</sub>, total Si content in the soil, including quartz, and all mineral and amorphous forms
- (2) Si<sub>O</sub>, poorly crystalline Fe oxides and short-range ordered aluminosilicates such as allophanes and imogolites which were extracted by the oxalate method
- (3) Si<sub>d</sub>, iron oxides extracted by the dithionite-citrate-bicarbonate method
- (4) Si<sub>CaCl2</sub>, soluble and bioavailable Si, extracted using the CaCl<sub>2</sub> method

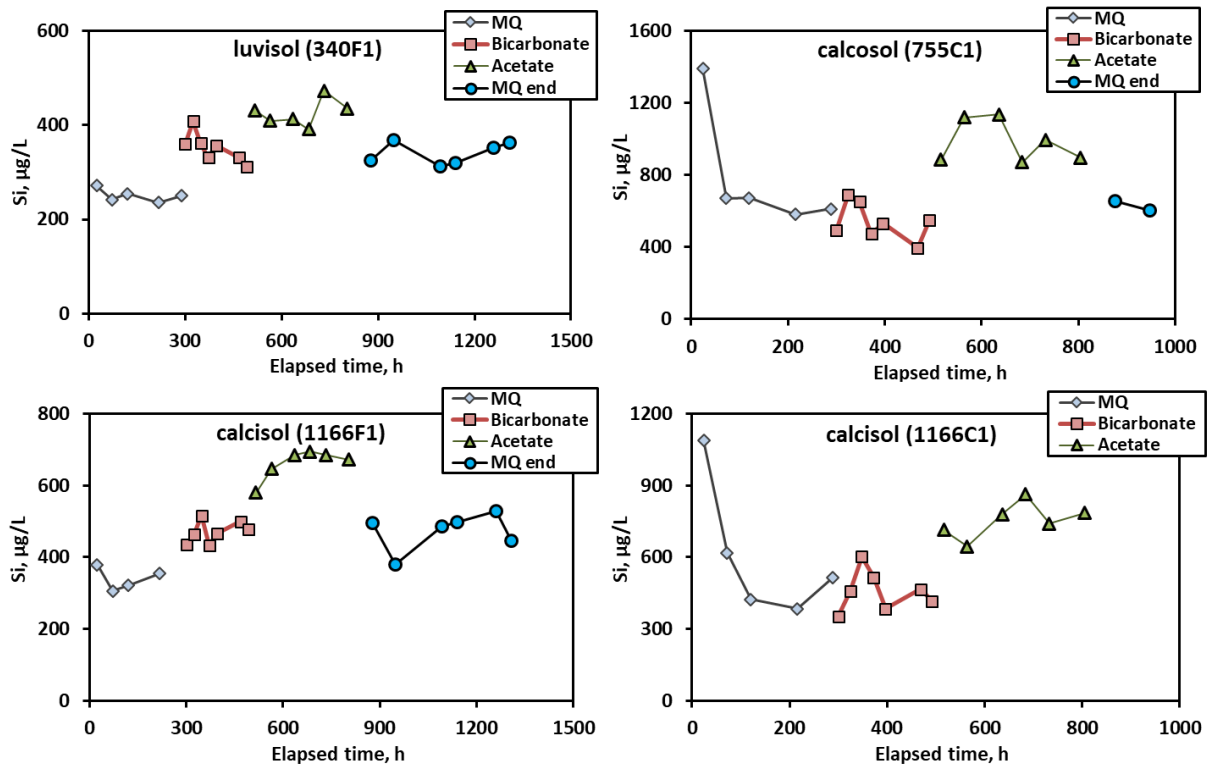


**A. Mixed-flow reactors**

**B. Flow-through column**

931  
 932  
 933  
 934  
 935  
 936  
 937  
 938  
 939  
 940

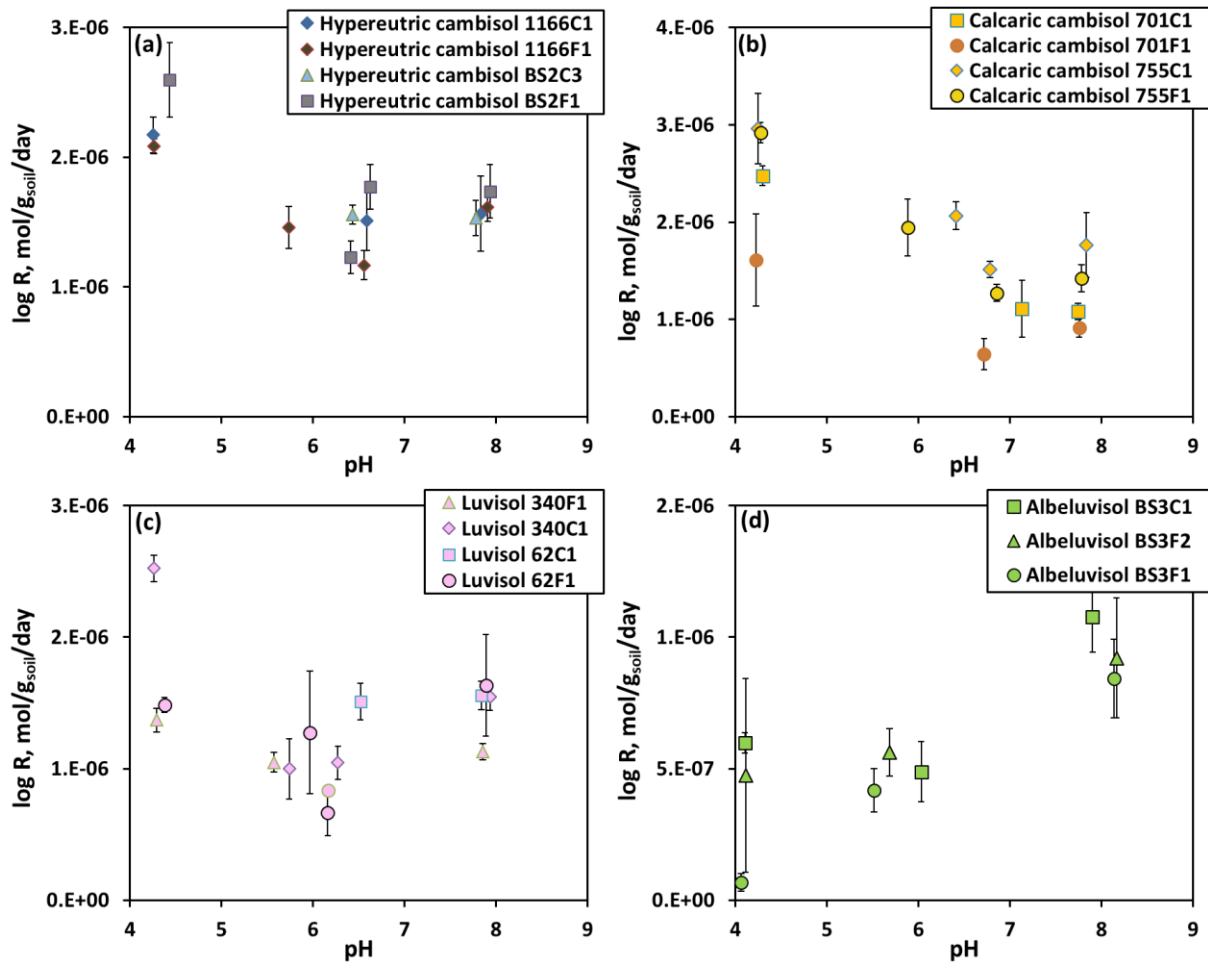
**Figure 1.** Experimental setup of mixed-flow reactors used for measurement of Si release rate from soils as a function of time and solution pH (A) and flow-through column experiments used for evaluating water-labile pool of adsorbed Si (B).



941  
942  
943

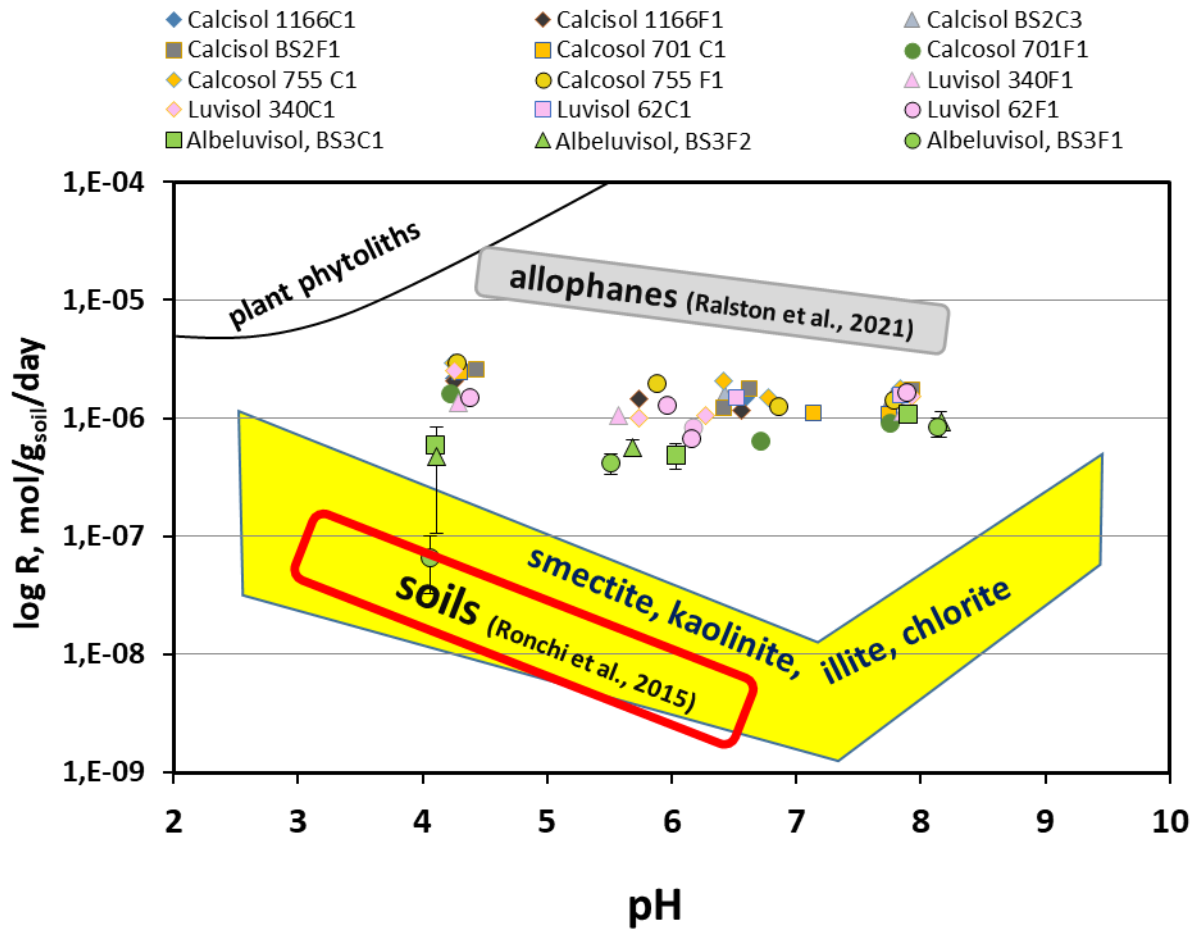
944 **Figure 2.** Examples of Si release pattern from different soils as a function of time, for  
945 different inlet solutions in the mixed-flow reactor. The inlet solutions were represented Milli-  
946 Q water at pH = 5.6, a mixture of 10 mM NaCl and 1 mM NaHCO<sub>3</sub> at pH = 8, and a mixture  
947 of 5 mM NaCl and 5 mM Acetic acid at pH = 4.2. The outlet pH values are listed in Table 2.  
948 For brevity, calcisol is used for hypereutric Cambisol and calcisol is for calcareic Cambisol.

949  
950  
951  
952  
953



954  
 955  
 956  
 957  
 958  
 959  
 960  
 961  
 962  
 963  
 964  
 965  
 966  
 967  
 968

**Fig. 3.** Si release rate from couple cultivated-forest soils hypereutric cambisol (A), calcaric cambisol (B), luvisol (C) and albeluvisol (D) in mixed-flow reactors plotted as a function of outlet solution pH.



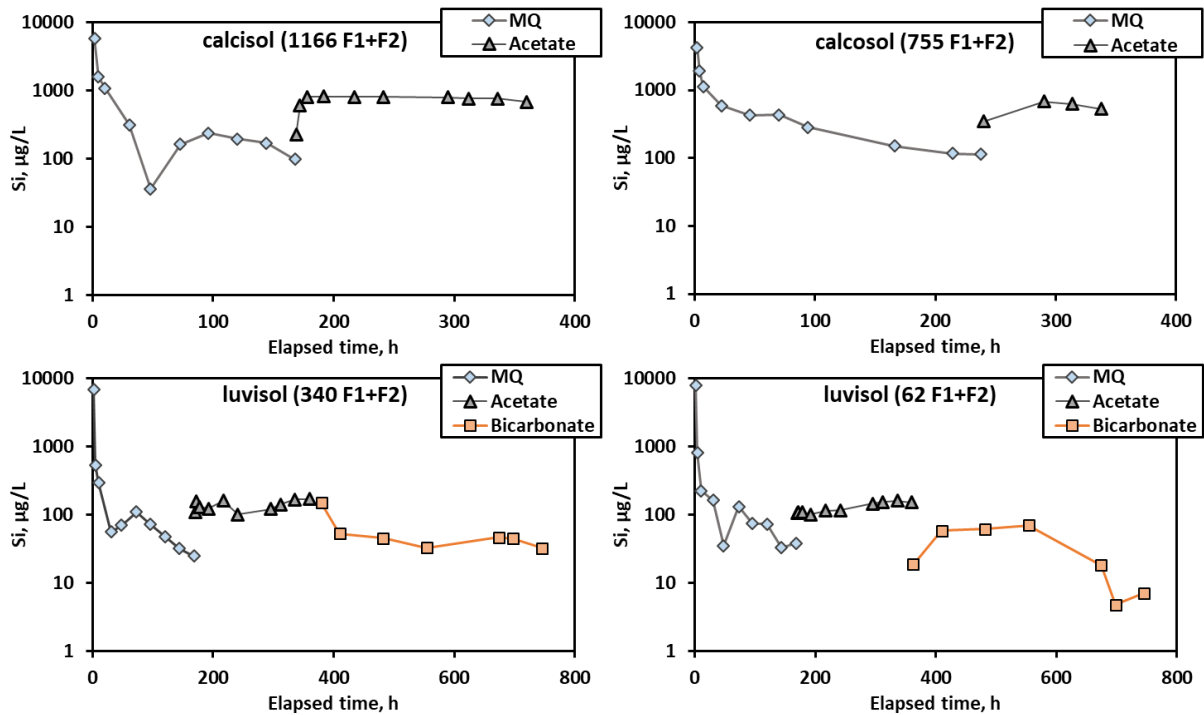
969  
970

971 **Figure 4.** Si release rates for typical soil clay minerals and studied soils as a function of pH at  
 972 25°C. Soil clays are represented by smectite (Golubev et al., 2006; Rozalen et al., 2008),  
 973 kaolinite and illite (Köhler et al., 2003, 2005) and chlorite (Lowson et al., 2005). Black solid  
 974 line represents dissolution rate of various plant phytoliths (horsetail, larch, fern) taken from  
 975 Fraysse et al. (2009). Red rectangle marks the range of Si release rate from columns with  
 976 forest and arable cambisols and luvisols (Ronchi et al., 2015). Grey rectangles denotes the  
 977 range of Si release rate of allophanes (Ralston et al., 2021).

978

979

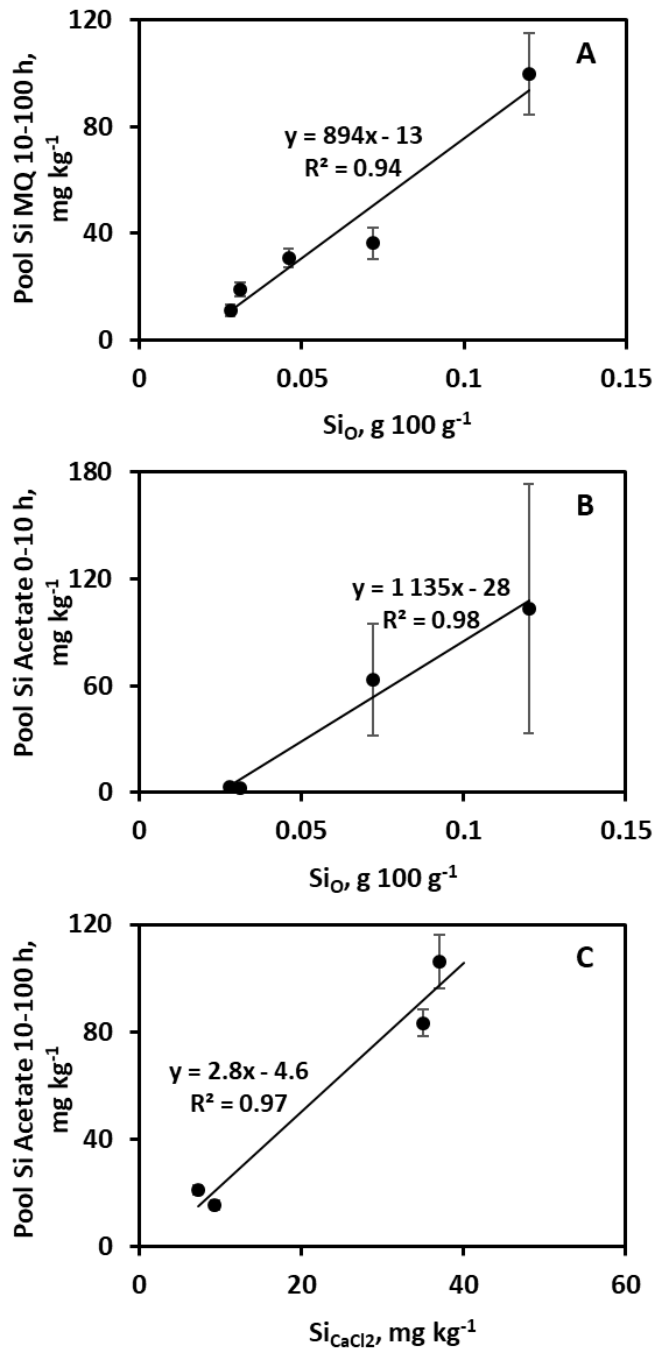
980



981  
 982  
 983  
 984  
 985  
 986  
 987  
 988  
 989  
 990  
 991  
 992  
 993  
 994  
 995  
 996  
 997

**Figure 5.** Examples of silica breakthrough curves in column experiments containing 1 g of surface and 3 g of intermediate horizons of forest soils. The initial (0-100 h) part of the curve was used to quantify the pool of water-labile Si present in the soil. For brevity, calcisol is used for the hypereutric Cambisol and calcosol denotes the calcaric Cambisol. Three inlet solutions were used in column experiments: Milli-Q water at pH = 5.6, a mixture of 10 mM NaCl and 1 mM NaHCO<sub>3</sub> at pH = 8, and a mixture of 5 mM NaCl and 5 mM Acetic acid at pH = 4.2. The outlet pH is listed in Table 3.





998  
999  
1000

1001 **Figure 6.** Correlations between pools of labile, fast-leaching Si measured in column filtration  
1002 experiments in this study with different Si forms in soils reported by Cornu et al. (2022). **A:**  
1003 MQ 10-100 h and Si<sub>O</sub>, silica linked to allophane/imogolites in the form of amorphous  
1004 coprecipitates with Fe/Al compounds as assessed by Tamm treatment; **(B):** acetate 0-10 h and  
1005 Si<sub>O</sub>; **C:** acetate 10-100 h versus Si<sub>CaCl<sub>2</sub></sub>, soluble bioavailable Si extracted with CaCl<sub>2</sub>.

1006  
1007  
1008